Diploma Thesis

Immune Response to ZX00 Implants in Healthy and Osteoporotic Rats

submitted by

Jan Eike Freudenthal-Siefkes

to obtain the academic degree

Doktor(in) der gesamten Heilkunde

(Dr^{in}. med. univ.)

at the

Medical University of Graz

executed at the

Department of Orthopaedics and Traumatology

under the guidance of

Priv.-Doz. Nicole Sommer, PhD

Graz, 08.01.2025

Staturory Declaration

I declare on my honor that I have written this thesis independently and without outside help, that I have not used any sources other than those cited and that I have identified the passages taken from the sources used verbatim or in terms of content as such.

Furthermore, I hereby declare that, if artificial intelligence (AI) tools were used to generate and/or correct certain text passages in the preparation of this thesis, this use was carried out in compliance with ethical principles, academic integrity and the guidelines of my university, and that this was subsequently made transparent and marked in an appropriate manner.

Graz, 08.01.2025 Jan Eike Freudenthal-Siefkes eh.

Acknowledgement

I would like to take this opportunity to thank all the people who have supported and motivated me through the ups and downs of writing my thesis. I would also like to thank all the members of the AG Weinberg who gave me my first insights into the world of research. My special thanks go to Priv.-Doz. Nicole Sommer, PhD, for her excellent supervision, her patience and support during the writing process and, above all, for all that I was able to learn from her in the course of this work. Finally, I would like to thank my parents - especially my mother, who has always been my support and whose support I could always be sure of.

Zusammenfassung in Deutsch

Hintergrund: In der EU wird eine von drei Frauen und einer von fünf Männern im Laufe ihres Lebens eine osteoporotische Fraktur erleiden. Dies entsprach 4,28 Millionen Fragilitätsfrakturen im Jahr 2019. Aufgrund der gestiegenen Lebenserwartung wird geschätzt, dass die Anzahl der Fragilitätsfrakturen bis 2034 auf 5,28 Millionen ansteigen wird. Die Osteosynthese von osteoporotischem Knochen stellt aufgrund von Veränderungen in den mechanischen, immunologischen und regenerativen Eigenschaften des Knochens eine besondere Herausforderung dar. Daher haben sich die Anforderungen an Implantatmaterialien hinsichtlich besserer Osteointegration, Osteokonduktivität und Osteoinduktivität geändert. Biologisch abbaubare Magnesium (Mg)-basierte Implantate, wie ZX00, zeigten vielversprechende Ergebnisse in Tierversuchen und ersten klinischen Anwendungen. Eine Studie an osteoporotischen Ratten zeigte jedoch eine beschleunigte Degradation des ZX00-Implantats. Daher war das Ziel dieser Studie, die systemischen osteoimmunmodulatorischen Veränderungen während der Osteoporoseentwicklung und die osteogenen Eigenschaften von ZX00 in einem Rattenmodell zu untersuchen. Wir analysierten in der ersten Phase der Studie die systemische immunmodulatorische Reaktion und die morphologischen Veränderungen des Knochens beim Auftreten von Osteoporose und in der zweiten Phase die systemische Immunantwort auf ZX00 unter osteoporotischen und gesunden Bedingungen, sowie das Degradationsverhalten von ZX00.

Methoden: Im ersten Teil wurden SD-Ratten ovariektomiert (OVX) und in Gruppen von je 5 Tieren zu den Zeitpunkten 4, 8 und 12 Wochen getötet. Das gleiche Verfahren wurde bei nicht ovariektomierten Kontrollgruppen angewendet. Blut-, Lymphknoten- und Milzproben wurden entnommen und eine quantitative FACS-Analyse der Immunzellpopulation durchgeführt. Die Tibiae wurden herausgeschnitten und *ex vivo* hochauflösende µCT-Aufnahmen erstellt. Basierend auf den µCT-Bildern wurden 3D-Rekonstruktionen der 12-Wochen-Gruppen erstellt und knochenmorphologische Marker wie BV/TV, Tb.Th, Tb.N, Tb.Sp und Conn.D analysiert. Im zweiten Teil wurden 40 SD-Ratten gleichmäßig auf die Gruppen OVX-ZX00, ZX00, OVX-sham und sham aufgeteilt. Zwölf Wochen nach der Ovariektomie wurden ZX00-Stifte implantiert und Scheinoperationen durchgeführt. Die Tiere wurden zu den Zeitpunkten 3 und 14 Tage

getötet. Blut-, Lymphknoten- und Milzproben wurden entnommen und eine quantitative FACS-Analyse der Immunzellpopulation durchgeführt. Tibiae wurden entnommen, in Technovit 9100 New eingebettet, und 100 µm dünne Schliffpräparate wurden nach Levai und Laczko gefärbt.

Ergebnisse: Wir beobachteten trabekulären Knochenverlust mit entsprechender Reduktion von BV/TV, Tb.N, und Conn.D wie auch einem Antieg von Tb.Sp bei den OVX-Ratten nach 12 Wochen. Die FACS-Analyse zeigte eine signifikant erhöhte T-Zell-Population zugunsten der CD4+ T-Zellen. Nach der Implantation von ZX00 wurde bei den ovariektomierten Ratten eine verstärkte Implantatdegradation beobachtet. Die FACS-Analyse offenbarte anfängliche Unterschiede zwischen Sham und OVX Ratten, die sich später angleichen, was auf einen ausgeprägteren Einfluss der Ovariektomie im Vergleich zur ZX00-Implantation hindeutet.

Schlussfolgerung: Alle Ergebnisse stützen eine lokale und systemische Wirkung der Ovariektomie, was auf ein proinflammatorisches Umfeld bei ovariektomierten Ratten hindeutet. Zusammengefasst war der systemische Effekt vor allem mit der Ovariektomie verbunden, ohne signifikante Veränderungen durch die Implantation von ZX00. Allerdings wären lokale Änderungen der Immunzellen und ein längerer Beobachtungszeitraum wünschenswert. Dies würde eine Abwägung der positiven immunmodulatorischen Effekte von Magnesium gegenüber den potenziellen negativen Aspekten einer schnelleren Implantatdegradation ermöglichen.

Abstract in Englisch

Background: In the EU, one out of three women and one out of five men will experience an osteoporotic fracture over their course of life. In 2019, 4.28 million osteoporotic-associated fragility fractures were reported. Due to increased life expectancy, the number of fragility fractures is estimated to reach 5.28 million by 2034. Osteosynthesis of osteoporotic bone presents a particular challenge due to alterations in the mechanical, immunological, and regenerative properties of the bone. Therefore, the requirements of implant materials changed to gain a better osseointegration, osteoconductivity, and osteoinductivity. Biodegradable magnesium (Mg)-based implants, such as ZX00, showed promising results in animal studies and in a first in-men study. Recently, results in osteoporotic rats revealed accelerated degradation of ZX00 compared to healthy rats. Hence, we aimed to investigate the systemic osteoimmunomodulatory changes during osteoporosis development and osteogenic properties of ZX00 in a rat model. Therefore, we assessed in the first phase of the study the systemic immunomodulatory response and the bone morphologic changes to the onset of osteoporosis and in the second phase the local morphogenic and systemic immune response to ZX00 in osteoporotic and healthy conditions.

Methods: First, SD rats were ovariectomized (OVX) and sacrificed in groups of 5 at the timepoints 4, 8, and 12 weeks. The same procedure was performed with the non-ovariectomized control groups. Blood, lymph node, and spleen samples were collected and quantitative FACS analysis of the immune cell population was performed. The tibiae were excised and *ex vivo* high resolution µCT was performed. After 3D reconstruction, morphologic markers BV/TV, Tb.Th, Tb.N, Tb.Sp, and Conn.D were analysed. Next, 40 SD rats were equally subdivided into the groups OVX-ZX00, ZX00, OVX-sham, and sham. Twelve weeks post ovariectomy, ZX00 pins were implanted and sham surgery was performed. The animals were sacrificed at the timepoints 3 and 14 days. Blood, lymph node, and spleen samples were collected and quantitative FACS analysis of the immune cell population was performed. Tibiae were excised, embedded in Technovit 9100 New and 100 µm thin-ground sections were stained after Levai and Laczko.

Results: We observed trabecular bone loss, with corresponding decreases in BV/TV, Tb.N, and Conn.D, as well as an increase in Tb.Sp in the OVX rats after 12 weeks. FACS analysis showed significantly elevated T cell population in favor of CD4+ T cells. After

ZX00 implantation, enhanced implant degradation was observed in the OVX rats. FACS analysis revealed initial differences between sham and OVX rats, which later aligned, indicating a more pronounced influence of the ovariectomy than the ZX00 implantation. **Conclusion:** All results support a local and systemic effect upon ovariectomy indicating to a pro-inflammatory environment in OVX rats. Taken together, the systemic effect was predominantly related to ovariectomy without significant changes after ZX00 implantation. However, local changes in immune cells and longer observation periods would be desirable. This allows for a weighing of the positive immunomodulatory effects of magnesium against the potential negative aspects of faster implant degradation.

Contents

List of abbreviations

ZX00	Mg-0.45wt%Zn-0.45%wtCa
PMOP	Postmenopausal osteoporosis
RANKL	Receptor Activator of NF-κB Ligand
RANK	Receptor Activator of NF-κB
OPG	Osteoprotegerin
IL	Interleukin
TNF	Tumor Necrosis Factor
M-CSF	Macrophage Colony-Stimulating Factor
FRAX	Fracture Risk Assessment Tool
SERM	Selective Estrogen Receptor Modulators
Ti	Titanium
Co	Cobalt
Cr	Chromium
Mo	Molybdenum
PLGA	Poly-lactide-*co*-glycolide
PLA	Polylactic acid
PCL	Polycaprolactone
PGA	Polyglycolic acid
Mg	Magnesium
WZ21	Mg–2%Y–1%Zn
ZX50	Mg–5Zn–0.3Ca
ZX20	Mg–2Zn-0.3Ca
ZX10	Mg–1Zn-0.3Ca
PROM	Patient Reported Outcome Measures
BMSCs	Bone Marrow Mesenchymal Stromal Cells
TLR	Toll-like Receptor
TCR	T cell Receptor
CD	Cluster of Differentiation

MHC	Major Histocompatibility Complex
IFN	Interferon
NK	Natural Killer Cell
G-CSF	Granulocyte-Colony Stimulating Factor
FACS	Fluorescence Activated Cell Sorting
μCT	X-ray Microtomography
SD	Sprague-Drawley
OVX	Ovariectomized
nOVX	Non Ovariectomized
BV/TV	Bone Volume Fraction
Tb.Th	Trabecular Thickness
Tb.N	Trabecular Number
Tb.Sp	Trabecular Separation
Conn.D	Connectivity Density
CGRP	Calcitonin Gene-Related Peptide
MgHA	Mg-incorporated Hydroxyapatite
IL-6Rα	Interleukin-6 Receptor α

List of tables

List of figures

1 Introduction

1.1 Osteoporosis

1.1.1 Economic burden

In the EU, one out of three women and one out of five men will experience an osteoporotic fracture over their course of life. In the population over 50 years of age, 22.1% of women and 6.6% of men are affected by osteoporosis (1). In absolute numbers, 32 million Europeans live with osteoporosis. The high prevalence of the disease led to a total of 4.28 million fragility fractures in 2019 (1). Due to increased life expectancy, the number of fragility fractures is estimated to reach 5.28 million by 2034 (1). In addition to the high mortality associated with fragility fractures, costs related to therapy and disability contribute to a significant economic burden. In 2019 the costs associated with osteoporotic fractures were estimated to be a total of 56.9 billion in the EU (1).

1.1.2 Osteoporosis effect on bone

Osteoporosis is defined by reduced bone mass and compromised microarchitecture, which increases fragility and susceptibility to fractures. It originates from an imbalance in the bone remodeling. Remodeling imbalance, characterized by an impaired bone formation response to increased activation of bone remodeling, is an essential component of the pathogenesis of osteoporosis (2, 3). The most relevant type of osteoporosis is primary osteoporosis, though the prevalence of secondary osteoporosis (caused by medication or primary disease (4)) actually grows. However, primary osteoporosis is subdivided into postmenopausal (PMOP) and senile osteoporosis. PMOP is characterized by estrogen deficiency, resulting in increased osteoclastogenesis. Senile osteoporosis is classified by reduced osteoblastogenesis due to aging.

The imbalance in bone remodeling is crucial in the pathogenesis of osteoporosis (2), mainly driven by the dysregulated RANKL/RANK/OPG axis (5).

Estrogen deficiency influences this axis via multiple pathways. Estrogen does not only promote the production of OPG, but also decreases the differentiation of osteoclasts by suppressing interleukin (IL)-1 and tumor-necrosis factor alpha (TNF-α), thereby inhibiting the release of M-CSF, RANKL, and IL-6. These pro-inflammatory cytokines are released

by various immune cells, which are upregulated due to the chronic inflammatory condition of estrogen deficiency (6).

1.2 Pharmacotherapy of osteoporosis

Table 1: WHO criteria of osteoporosis. SD: Standard variation

Defintion	T score
Normal	>-1 SD
Osteopenia	-1 to -2.5 SD
Osteoporosis	≤-2.5 SD
Severe osteoporosis	≤-2.5 SD plus fragility fractures

The indication for pharmacotherapy is established by multiple factors. The basis is the T score, a measurement of the bone mineral density in relation to the mean of a cohort of healthy 20 to 29-year-old individuals (7), ranging from -1 to -2.5 for osteopenia and ≤-2.5 for osteoporosis (Table 1) (8). Additionally, spinal and extraspinal fractures define the severity of the osteoporosis (9). The general limit value for pharmacotherapy is set at a T score of -2.5 (10). Since several additional factors, such as smoking, alcohol consumption, therapy with glucocorticoids or chronic inflammatory diseases, increase the fracture risk substantially, multifactorial risk calculation scores, like the Facture Risk Assessment Tool FRAX, have been established (11). Current concepts to pharmacologically treat osteoporosis address decreased bone density and structural deterioration with two mechanisms – antiresorptive and osteoanabolic (12). Antiresorptive drugs are bisphosphonates, Denosumab, and Raloxifene (13).

However, the primary root to treat osteoporosis are bisphosphonates. Bisphosphonates exert their antiresorptive effect by inhibiting osteoclast activity and promoting osteoclast apoptosis. In case of bisphosphonate intolerance or wearing-off the monoclonal antibody, Denosumab is alternatively used. Denosumab acts as a decoy receptor for RANKL, similarly to OPG, thereby reducing osteoclast activity (13). Moreover, the second line therapy for postmenopausal osteoporosis is the selective estrogen receptor modulator (SERM) Raloxifene, which mimics estrogen's protective actions against bone loss, while minimizing the risks associated with estrogen (10, 13). In cases of severe osteoporosis, drugs with osteoanabolic o dual-action effects are indicated. Therefore, Teriparatid or Romosozumab is used (10). Teriparatid acts exclusively in an osteoanabolic manner by

increasing calcium resorption/phosphate excretion in the kidney and stimulating vitamin D3 synthesis. Romosozumab is a dual-action drug: while increasing bone formation by promoting osteoblast differentiation and activity, bone resorption is decreased by osteoclast inhibition. The use of Romosozumab is highly limited due to wearing-off within 6 months (10). Although research gained advanced understanding regarding the development of osteoporosis over the last few years, there is still considerable potential for improvement. Especially, to understand and investigate the bilateral role of the immune system and osteoporosis is of great interest and is mainly referred to as osteoimmunology (14, 15). Accordingly, pharmacotherapy improved by contributing potent inhibitors of bone resorption and stimulators of bone formation. Nevertheless, there are still limitations pertaining therapy adherence, efficacy on non-vertebral fractures, and wearing-off of drugs coupled with long-term adverse events (16). In pharmacotherapy, the problem of paired osteoblast and osteoclast function remains unsolved. Inhibition of osteoclasts reduces bone formation and in reverse (17). The issue of boundaries of pharmacotherapy is supplemented by an underdiagnosis of the disease and undertreatment. As a result, the incidence of osteoporosis-related fractures remains elevated, sustaining a significant demand an surgical interventions (18).

1.3 Osteosynthesis

The two central principles of osteosynthesis are interfragmentary compression and adaption of the fractured bone segments. The application of these principles is achieved by extramedullary and intramedullary implants (19). Depending on the technique, commonly used implants include plates, screws, intramedullary nails, and wires (20). By reducing physiological load or transferring it to the surgically introduced load-bearing device, compressive, bending, or torsional forces acting on the central primary fragment are transmitted to the peripheral fragment across the fracture gap. In cases of large substance defects, the use of bone substitute materials may be necessary. Osteosynthesis' materials should remain in place for at least one year to ensure load-bearing stability of the fractured bone. This applies to devices, such as plates or intramedullary locking nails. In principle, modern implants can remain in the body for a lifetime. However, patients often experience discomfort, which may necessitate removal of the implant (20-22).

1.3.1 Standard materials

In modern osteosynthesis procedures, the use of temporarily implanted devices has become indispensable. The demands for high biocompatibility and load-bearing property limit the choice of implant material to metals and alloys (20). Major aspects of biocompatibility are osteobiologic properties, such as osteogenicity, osteoconduction, and osteoinduction (23).

Commonly used metals include iron, nickel, cobalt, titanium (Ti), molybdenum, and zirconium. Various alloys of these metals can meet different requirements for strength, elastic modulus, and corrosion resistance (24). Currently, stainless steel, Ti-based alloys, and cobalt-based alloys are the predominantly used materials for implant devices (25). Stainless steel possesses several favorable properties, such as high wear resistance, good fatigue resistance, and low costs. It is also non-toxic and biocompatible, as it does not elicit any adverse reactions from surrounding tissues. Although, in rare cases, patients show allergies to chromium or nickel. Moreover, stainless steel tends to crevice and pitting corrosion and stress shielding (26-28). Stainless steel implant devices dominated the market due to low costs. However, the proportion of mainly Co/Cr/Mo and Ti alloys continuously grows. Co-Cr-based alloys offer high corrosion resistance, excellent wear resistance, biocompatibility, and superior load-bearing properties. This is counterbalanced by an increased risk of early implant loosening (26, 29). The use implant devices made of Ti and its alloys became more popular due to favorable mechanical properties, low weight , biocompatibility, and resistance to wear and corrosion. These materials have the disadvantage of partially low shear strength, unfavorable tribological properties, and particularly high costs (26, 30, 31). In general, traditional metal implants lack certain properties, because of non-degradability and necessity for removal surgery (32). Stress shielding and bone loss over time that is caused by mechanical shunting might occur due to the use of standard metal implants (33, 34). Furthermore, standard metal implants have substantial limitations in the management of osteoporotic fractures, femoral head necrosis, and large bone defects (35).

1.3.2 Synthetic polymers

Synthetic polymers are subdivided into biodegradable and non-degradable (36). In particular, degradable synthetic polymers are of interest in orthopedic trauma surgery, as they can help to avoid the need for a second operation (37). As an alternative to traditional orthopedic metal implants, synthetic polymers, including Poly-lactide-*co*-glycolide (PLGA), polylactic acid (PLA), polyglycolic acid (PGA), and polycaprolactone (PCL), have been increasingly used in orthopedic procedures (38). These synthetic polymers have favorable biocompatibility compared to conventional metal implants. Nonetheless, synthetic polymers have several limitations, such as the presence of toxic residual monomers, low wear resistance, and accumulation of acidic degradation intermediates, causing pathological bone resorption. Additionally, their suboptimal mechanical properties restrict their broader clinical application. In osteoporotic fractures, the performance of synthetic polymers is as limited as those of standard metals (35, 39).

1.3.3 Magnesium-based implants

The first reported use of magnesium (Mg) in a surgical context was by E.C. Huse in 1878. Huse used Mg-based ligatures and observed its degradable properties (40). Around 1900, the surgeon Erwin Payr from Graz recognized the versatile applications of biodegradable Mg in surgery. His work inspired many researchers and physicians to further explore this material (41, 42). The use and research of Mg in osteosynthesis on a broader scale were reported by Lambotte in 1932 (43). In the 2000s, the Helmholtz-Zentrum Geesthacht in Germany and the Chinese Academy of Sciences Institute of Metal Research in China became particularly prominent in the research of Mg-based implants for osteosynthesis. These research groups focused on the development of Mg alloys with enhanced corrosion resistance and biocompatibility to enable their clinical application (28, 44). Biodegradable Mg displays high biocompatibility and the e-modulus is close to human bone (45, 46), which reduces the risk of stress shielding (47, 48). Nevertheless, Mg implants exhibit fast degradation rates and the release of large amounts of hydrogen gas during the degradation (49-51). To slow down the degradation rate, chemical elements, such as Aluminium, Manganese, Zinc, Calcium, Lithium, Zirconium, and Rare Earth Elements (e.g. Yttrium- Y or Gadolinium- Gd) are industrially used to influence the mechanical and physical properties of Mg alloys (47). For instance, alloying with Gd showed promising

results in *in vitro* immersions tests regarding slow degradation rates (52-54). However, an accumulation of Gd was observed in several organs of Sprague Dawley rats (55). The Y-containing alloy WZ21 showed a slow degradation (56). The study also investigated ZX50, a Zn-containing alloy. ZX50 displayed a high degradation rate, and temporarily, a massive gas formation (56) that might reduce bone formation (57). In contrast, the chemical elements, Mg, Ca, and Zn, contained in ZX alloys are essential minerals of the human body, and thus, degradation particles pose no toxicity concern (58). The comparison of ZX10 and ZX20 demonstrated that adjusting the Zn content is a suitable method to modify the degradation rate (59). In a large animal study by Holweg et al., a lean alloy Mg–0.45Zn–0.45Ca in wt% (ZX00) displayed suitable properties regarding mechanical strength and degradation rate without interfering with fracture consolidation (60). The first applications in humans demonstrated promising mid-term results regarding patient-reported outcome measures (PROMs), functional outcomes, and implant degradation as observed in radiographic imaging (61, 62). During the degradation process, Mg^{2+} ions are released. Mg^{2+} ions are non-toxic and actually enhance bone regeneration by promoting the differentiation of various osteogenic cells and suppressing osteoclasts activity (63, 64). This was also demonstrated by elevated bone mineral apposition rates surrounding degrading Mg-based implants, along with an increase in bone mass (65). The beneficial effect of Mg^{2+} is dose-depended; low to medium concentrations promote bone formation by enhancing osteogenesis of BMSCs (66, 67), whereas high concentrations appear to inhibit mineralization (68, 69). Furthermore, several *in vivo* studies indica ted enhanced angiogenesis in bone regeneration (70, 71). Mg^{2+} ions induced macrophage phenotype transformation in favor for anti-inflammatory M2 macrophages and promoted the release of anti-inflammatory cytokines by inhibiting the TLR-NF-κB signaling pathway (67, 68, 72-75). Moreover, Mg enhances T cell activation (76), particularly Th1 and Th2 (77).

1.4 Immune system

The immune systems consist of an innate (non-specific) and an adaptive (specific) part. Both operate in an interplay of cellular and humoral components, which are predominantly distinct from each other.

1.4.1 Innate immune system

Monocytes/macrophages, mast cells, natural killer cells, and granulocytes subdivided into neutrophils, eosinophils, and basophils constitute the cellular component of the innate immune system. Lysozyme, acute-phase proteins, cytokines, and the complement system constitute the humoral component.

The innate non-specific defense is effective against various microorganisms and shows species differences against different pathogens. Under certain circumstances, such as trauma or chronic inflammatory conditions, the innate immune system also aims for endogenous cells (78, 79). The ability to differentiate between foreign and endogenous cells is created by toll-like receptors, which detect specific surface structures on bacteria and viruses (79). Once bacteria or foreign bodies have entered the body, elimination takes place by phagocytizing cells including polymorphonuclear, neutrophilic granulocytes of the blood and the mononuclear phagocytes found in blood and tissues (79). If pathogenic germs have penetrated body tissue during an injury, leukocytes migrate out of the bloodstream (extravasation) to enter the site of tissue damage. The extravasation is initiated by the secretion of inflammatory mediators from tissue-resident macrophages in the affected site. This results in leukocyte-endothelial interaction and the adhesion of leukocytes to the endothelia (78). The adhered leukocytes migrate chemotactically through the vascular wall toward the inflammation site. The migration is initiated and sustained by chemokines, a subgroup of cytokines (78).

Once neutrophil granulocytes or macrophages successfully migrate into the inflammatory site, phagocytosis begins. Phagocytes capture pathogens by attaching to their membrane surface. Following attachment, the phagocytes form pseudopodia that envelop the foreign body, leading to the formation of phagosomes. The degradation of the pathogen starts when the phagosomes fuse with lysosomes to form phagolysosomes (80).

Opsonization markedly enhances the phagocytic activity of phagocytes. Pathogens are marked with antibodies or complement factors to facilitate identification and elimination by the immune system (80-82).

1.4.2 Adaptive immune system

T and B cells constitute the cellular component of the adaptive immune system, whereas antibodies and cytokines form the humoral component.

The body's adaptive defense system precisely recognizes and eliminates foreign molecular structures known as antigens. This acquired immunity is primarily supported by cells, and characterized by the high specificity in recognizing antigens. This immunological memory and the ability to discern between self and non-self molecular structures accurately enables targeted protection while minimizing harm to the host (80, 82).

T precursor cells exiting the bone marrow initially lack both the T cell receptor (TCR) and the CD4 and CD8 co-receptors. After the cells are transported to the thymus, T precursor cells mature and acquire their TCR. In addition to the TCR, CD4, and CD8 co-receptors are synthesized within each T cell in the subcapsular zone of the thymus. The T precursor cells without TCR, CD4, and CD8 (termed double-negative thymocytes) develop into double-positive thymocytes, expressing both CD4 and CD8 along with their TCR. These double-positive (CD4+ and CD8+) thymocytes migrate to the cortical region of the thymus and undergo positive and negative selection. Positive selection of T-cells occurs in the thymus, ensuring their ability to recognize self- major histocompatibility complex (MHC) molecules.

MHC I molecules present endogenous antigens to CD8+ T cells, initiating cytotoxic responses. MHC II molecules present exogenous antigens to CD4+ T cells, initiating T cell activation.

Negative selection eliminates autoreactive T-cells, preventing autoimmune diseases. These mechanisms ensure the development of functional, self-tolerant T-cells. During the selection process, the thymocytes lose either the CD4+ or CD8+ co-receptor. Upon completion of the maturation process, thymocytes migrate to secondary lymphatic organs. They reside as naive T cells, awaiting activation by contact with antigens. After stimulation by an antigen, CD4+ T cells differentiate into T helper cells and CD8+ T cells into cytotoxic T cells (78, 80).

B cells are responsible for the specific humoral immune defense. Precursor cells mature in the bone marrow into naïve B cells. On the surface of the B cells are receptors located. These receptors are membrane-bound antibodies. The Activation of the naïve B cells is either independent or T cell-mediated.

Both pathways facilitate the differentiation of B cells into plasma cells. In the T cell-independent pathway, the antigen binds directly to the B cell. Conversely, in the T cell-dependent pathway, the antigen is phagocytized and presented to the B cell by a T helper cell. The T cell-dependent mechanisms generate a significantly more efficient immune response and additionally establish immunological memory. A small proportion of T-effector cells and antibody-producing plasma cells can survive for many years in the body as T or B memory cells. A certain concentration of antibodies can be detected, even without an antigen stimulus. In the event of a re-infection with the same structure, memory cells can be activated directly by the pathogen much more rapidly than inactive cells since the maturation processes are already complete (78).

1.4.3 Local inflammatory response

An acute inflammation can be triggered by biological, chemical, and physical noxae, such as trauma resulting from tissue injuries or surgical interventions, as well as by necrotic cell death due to ischemia. Typically, this leads to the local migration of neutrophil granulocytes into the tissue. Subsequently, monocytes also migrate to the site, where they differentiate into macrophages. Both neutrophils and macrophages then eliminate bacteria, foreign bodies, or destroyed autologous material through phagocytosis (79, 80).

1.4.4 Systemic inflammatory response

Systemic inflammatory responses are generally associated with an increase in white blood cell count, primarily driven by an increase in the number of neutrophils in the peripheral blood. This increase, termed neutrophilia, results from enhanced production and release of neutrophil granulocytes from the bone marrow into the peripheral blood, along with a delayed apoptosis of these cells. The release of younger neutrophils shifts the distribution between young and older segmented neutrophils, known as a left shift in the distribution (80, 82).

1.5 Lymphatic organs

Lymphatic organs are organs or tissue sections where lymphocytes differentiate or proliferate. The different function divides them into primary and secondary lymphatic organs.

1.5.1 Primary lymphatic organs

Primary lymphatic organs include the bone marrow and thymus. In these organs, lymphocytes differentiate from stem cells, proliferate, and mature (80). The stem cells for all blood cells, including lymphocytes, are located in the bone marrow. T cells leave the bone marrow early and mature in the thymus, where they acquire the ability to distinguish between self and non-self-antigens. B cells remain in the bone marrow longer to undergo an initial phase of their development. Here, B cells acquire specific antigen receptors that enable them to respond to antigens. B-lymphocytes acquire the ability to distinguish between self and non-self in both, primary and secondary lymphatic organs (81).

1.5.2 Secondary lymphatic tissue

The primary interception sites for pathogenic microorganisms are the secondary lymphatic organs, which include the spleen, lymph nodes, tonsils, and lymphatic tissues associated with the bronchi and intestines (83). These organs specialize in facilitating encounters between T cells and B cells with their specific antigens. Antigens reach these secondary lymphatic organs either through the afferent lymph flow or, are captured in the tissue by roaming dendritic cells, which, once loaded with antigens, migrate to these organs. Dendritic cells process these antigens and present them to the immunocompetent lymphocytes within the secondary lymphatic organs. The proliferation of these immunocompetent lymphocytes in these organs subsequently leads to the macroscopically observable swelling of lymph nodes or spleen enlargement during an infection (84). Additionally, macrophages of the mononuclear phagocytic system, stationed in many exposed organs such as the lung alveoli, joint spaces, spleen, lymph nodes, and brain. These tissue-resident macrophages play a role in detecting foreign antigens (80, 81).

1.6 Immune cell's role in osteoporosis

T cells

CD8+ T cells are a subset of T cells, also referred as cytotoxic T cells, fulfilling an important role in cell-mediated immune responses.

In this role, CD8+ T cells are responsible for regulating immune responses while also eliminating infected or mutated cells by lytic and non-lytic processes (85, 86).

The current state of research offers no evidence regarding the involvement of CD8+ T cells in the pathogenesis of osteoporosis. Although this subset of Tregs is CD8+, the larger proportion in humans and rodents is CD4+ (87). Besides their general function of maintaining immunological self-tolerance and modulation of immune response, the bone-specific function is suppression of osteoclastogenesis (14). CD4+ T-helper cells interact with other immune cells through surface receptors and secreted cytokines. Subtype Th1 stimulates macrophages and therefore osteoclastogenesis (88), while subtype Th2 stimulates B cells, mast cells, and granulocytes (89). Furthermore, T-helper cells are subclassified by their cytokine profile and receptor expression. Among these subtypes, Th1, and Th17 play a pivotal role by secreting TNF-α and IL-6 to stimulate osteoclastogenesis via RANKL. (88). Moreover, interferon (IFN)-γ is secreted by CD4+ and CD8+ T cells as well as natural killer (NK) cells and inhibits osteoclasts (90).

B cells

The role of B cells is context-dependent. While B cells play a crucial role in inhibiting osteoclasts through the secretion of OPG receptor decoys, inflammatory environments can shift the effect of B cells on bone remodeling towards bone resorption (91). Estrogen deficiency leads to an increase of B cells (92). Under inflammatory conditions, B cells secrete RANKL, which promotes the activation of osteoclasts (14, 93, 94). B cells in inflammatory environments also produce granulocyte colony-stimulating factor (G-CSF), which results in the proliferation of osteoclast progenitors. Additionally, G-CSF can upregulate neutrophil infiltration, which promotes inflammation (95).

Granulocytes

Neutrophil senescence is implicated in various health conditions, including osteoporosis (96). several mechanisms were proposed to link neutrophil senescence and disrupted bone metabolism. One concept is the predictive value of the neutrophil-to-lymphocyte ratio. Older individuals often exhibit elevated circulating neutrophils, connected to changes in the pathways that regulate apoptosis. When neutrophils do not undergo apoptosis as expected, they accumulate, resulting in a higher neutrophil-to-lymphocyte ratio that is associated with osteoporosis (97). In postmenopausal conditions, the regulation of neutrophil activation, chemotaxis, and the production of reactive oxygen species is impaired by estrogen deficiency (98). There is a reduced mobilization of neutrophils to inflammation sites, resulting in CD4+ T cells secreting cytokines like IL-17, inducing osteoclastogenesis (99). Moreover, neutrophils influence bone homeostasis by affecting the differentiation into osteoblasts, neutrophils also inhibit the secretion of extracellular (98).

Eosinophils contribute to osteoporosis by releasing osteoclastogenic cytokines like TNF-α, IL-6, and IL-31 (100, 101). In mice, high eosinophil numbers can effectively protect against postmenopausal and inflammatory bone loss by inhibiting osteoclast activity and maintaining bone mass. The amplification of bone loss was observed in conditions of impaired eosinophil function (102).

Monocytes/Macrophages

The primary functions of macrophages are phagocytosis and the induction of inflammatory responses. Macrophages are differentiated into tissue-resident or differentiated from blood monocytes, as a response to an inflammatory signal.

Tissue-resident macrophages possess adapted properties customized to their location. Bone-specific macrophages include bone marrow macrophages, osteoclasts, and osteal macrophages (103).

Furthermore, macrophages are divided based on their general function. M1 macrophages are related to the exacerbation of inflammation and are therefore characterized by the expression of proinflammatory cytokines. On the other hand, M2 macrophages are linked to anti-inflammatory reactions mediated through the expression of anti-inflammatory

cytokines (104). Additionally, M2 macrophages promote the differentiation of precursor cells into osteoblasts and hence bone formation (105, 106).

Activated monocytes or bone marrow macrophage precursors adhere to the bone surface to form multinucleated osteoclasts. The proliferation and differentiation into osteoclasts are primarily stimulated by M-CSF and RANKL (107). Estrogen can inhibit the RANKL stimulation of M2 macrophages. As a result, estrogen deficiency promotes the differentiation of macrophages into osteoclasts (108).

Activated, macrophages possess osteoclastogenic properties by expressing pro-inflammatory cytokines such as IFN-γ, TNF-α, and IL-1 (109).

2 Hypothesis and Aims

The increasing prevalence of osteoporosis not only leads to a higher incidence of fractures but also complicates osteosynthesis due to reduced bone mineral density and impaired bone regeneration (1, 2). To address this challenge, research into new implant materials has been pursued. Biodegradable magnesium (Mg)-based implants, such as ZX00, showed promising results in animal studies and initial clinical applications (110, 111). Previously, ZX00 was investigated in an ovariectomy-induced osteoporotic rat model, indicating enhanced ZX00 degradation when compared to old and juvenile healthy controls. Interestingly, ZX00 implant volume was significantly reduced even after 2 weeks post-surgery. Sommer et al. suggested an osteoporosis-linked low-grade inflammation that might change the pH locally, thereby enhancing the degradation rate of ZX00 (112). However, the impact of the immune system and low-grade inflammation on Mg implant degradation under osteoporotic conditions still needs further investigation.

Accordingly, this study aimed to investigate the systemic osteoimmunomodulatory changes during osteoporosis development and osteogenic properties of ZX00 in a rat model.

Therefore, we assessed

(i) the systemic immunomodulatory response and the bone morphologic changes to the onset of osteoporosis

(ii) the systemic immune response to Mg-based implant (ZX00) in osteoporotic and healthy conditions and implant in-growth.

To test the hypothesis, SD rats were ovariectomized (OVX) and sacrificed in groups of 5 at the timepoints 4, 8, and 12 weeks. The same procedure was performed with the non-ovariectomized control groups. Blood, lymph node, and spleen samples were collected and quantitative FACS analysis of the immune cell population was performed. The tibiae were excised and *ex vivo* high resolution µCT was performed. Based on the µCT-images 3D reconstructions of the 12 weeks groups were created and bone morphologic markers BV/TV, Tb.Th, Tb.N, Tb.Sp, and Conn.D were analysed.

In the second part, 40 SD rats were equally subdivided in the groups OVX-ZX00, ZX00, OVX-sham, and sham. 12 weeks post ovariectomy ZX00 pins were implanted and sham surgery was performed. The animals were sacrificed at the timepoints 3 and 14 days.

Blood, lymph node, and spleen samples were collected and quantitative FACS analysis of the immune cell population was performed. Tibiae were excised, embedded in Technovit 9100 New and 100 µm thin-ground sections were stained after Levai and Laczko.

3 Material and Methods

3.1 Ethical statement

Small animal studies were approved by the Austrian Federal Ministry for Science and Research and followed the guidelines on accommodation and care of animals formulated by the European Convention for the Protection of Vertebrate Animals Used for Experimental and Other Scientific Purposes (GZ number: 2021-0.236.683).

3.2 Material development

The purified Mg was alloyed with Zn and Ca to synthesize the alloy Mg<0.5 wt%Zn<0.5wt%Ca. After solution and aging heat treatments, indirect extrusion was performed at 325 C. Subsequently, pins were machined using polycrystalline diamond tools, taking special care to avoid any kind of surface contamination. Pins were then cleaned using ultrasonic waves, air dried in clean-room atmosphere and packaged airtight. Sterilization was performed by gamma irradiation (minimum dose 25 kGray).

3.3 Animals and surgery

Four-weeks old Sprague Dawley rats were purchased from Janvier Labs and housed at MUG (Biomedical Research Facility) under conventional conditions with free access to food (normal chow diet) and water, up to 9 months of age (skeletally mature (37) female SD rats). At 9 months of age, rats underwent ovariectomy (OVX) or served as healthy controls (Ctrl) as described by (112).

3.3.1 Ovariectomy

Volatile isoflurane (Forane®, Abbot AG, Baar, Switzerland) was administered for general anesthesia preceded by subcutaneous combined sedation, administering a mixture of Fentanyl (20 µg kg−1 Fentanyl®, Janssen-Cilag GmbH, Neuss, Germany), Midazolam (400 µg kg−1 Midazolam Delta®, DeltaSelect GmbH, Dreieich, Germany) and Medetomidine (200 µg kg−1 Domitor®, Pfizer Corporation Austria GmbH, Vienna, Austria) via intraperitoneal injection. After disinfection, an incision was made along the middle line of their respective abdomens. Rats from the ovariectomy (OVX) group were sutured layer

by layer after complete removal of the bilateral ovaries. The general anesthesia will be then antagonized by an intraperitoneal injection of a mixture of Naloxone (120 lg kg1 ; Narcanti, Torrex Chiesi Pharma GmbH, Vienna, Austria), Flumazenil (50 lg kg1 ; Anexate, Roche Austria GmbH, Vienna, Austria) and Atipamezole (250 lg kg1 ; Antisedan, Pfizer Corporation, Vienna, Austria). Postoperatively all animals received 200 mg kg1 Caprofen (Rimadyl, Pfizer Corporation, Vienna, Austria), which was subcutaneously injected on the day of operation to ensure analgesia. During the first postoperative week (up to the seventh day) analgesia maintained by administration of 60 mg Piritramid (Dipidolor; Janssen-Cilag GmbH, Neuss, Germany) in 40 ml 5% glucose added to 500 ml drinking water. Postoperatively the rats were allowed to move freely in their cages without external support and unrestricted weight bearing. Daily clinical observation was performed throughout the study period.

3.3.2 Transcortical implantation

Three months after ovariectomy (12-months of age) rats underwent transcortical implantation (n=40 rats). Therefore, both hind legs were shaved, antisepticized with alcohol pads, and dried. A skin incision (length, 1-2 cm) was made medial over the proximal lateral tibial metaphysis, cleared from blood and connective tissue. For the sham- and ZX00 groups, a drill (1.55 mm) with ascending diameter (Synthes, Paoli, PA, USA) was used to prepare the bicortical implantation bed. Drilling was performed at a low rotational speed of 200 rpm and profuse physiological saline irrigation will be applied using a syringe in order to minimize frictional heat and thermal necrosis. For the ZX00 groups, the cylindrical implant (l=8 mm, d= 1.6 mm) was inserted by gentle tapping, resulting in a uniform press fit. The operating field was irrigated thoroughly with physiological saline solution and the wound was closed. The general anesthesia was then antagonized according to the section “ovariectomy”.

3.3.3 Euthanasia and tissue collection

After 3 and 14 days post-implantation/post-sham-surgery, 5 animals per group were euthanized with 25 mg sodium thiopental (Thiopental® Sandoz, Sandoz GmbH, Kundl, Austria) by injection into the cardiac ventricle leading to immediate cardiac arrest. Blood

will be drawn and plasma will be isolated for systemic analysis. Blood, tibiae, lymph nodes and spleen were explanted. Blood, lymph nodes and spleen were subsequently processed for cell isolation used in flow cytometry.

3.3.4 *Ex vivo* micro-computed tomography (µCT)

All excised tibiae underwent e*x vivo* high-resolution (~10µm per voxel) micro-computed tomography (µCT) using a Bruker Skyscan 1276 device.

3D reconstruction of bone, implant and gas volume was performed to quantify the following parameters using CTAn and CTVox Software: BV/TV, Tb.N, Tb.Th and Tb.Sp.

3.3.5 Flow cytometry

Single-cell suspensions of blood, lymph nodes, and spleens were used for subsequent flow cytometric staining and analysis. For all groups, blood, lymph nodes, and spleens were excised and subsequently processed for cell isolation. In brief, total blood (~5-10 ml) was drawn, 3.8% sodium citrate was added to avoid coagulation and stored at 4°C. For red blood cell lysis, 1x RBC buffer (1:20) was mixed with 1 ml blood. After centrifugation, this step was repeated. 300 µl of cell lysate (in DMEM; complete medium) was prepared for flow cytometry. For lymph nodes and spleens, tissues were collected and placed in DMEM. placed on a 100 µm pore cell strainer and crush with the end of a syringe piston. The cell strainer was washed with 1xPBS. For spleens, red blood cells were lysed with RBC buffer. After centrifugation, cell pellets were resuspended in complete medium and 300 µl were prepared for flow cytometry.

3.3.6 Hard tissue embedding and histology

According to the protocol established by Willibold and Witte (39), metaphyseal area of tibiae were embedded in Technovit 9100 (Technovit® 9100, Heraeus Kulzer, Frankfurt, Germany).

Embedded samples were grinded to gain 100 µm slices for Levai-Laczko staining according to (112).

3.3.7 Statistical Analysis for all measurements

For statistical analysis, GraphPad Prism 9 was used. To investigate differences between OVX and Ctrl in regard of bone quality, unpaired t-test was used, although sample size was below 10. In order to compare to literature, results are given as mean ± standard deviation (SD). To investigate differences between differently treated (ZX00 or sham) OVX and Ctrl at different time points, two way ANOVA was performed. A p-value < 0.05 will be considered statistically significant.

4 Results

4.1 Bone morphology is altered upon ovariectomy in rats

OVX and Ctrl animals were sacrificed 4, 8 and 12 weeks post-ovariectomy. Tibiae were excised to undergo *ex vivo* high-resolution µCT. Images were 3-dimensionally reconstructed and histomorphometrical analysis was performed within a 700 µm region of interest. Therefore, cortical and trabecular bone were separated and prominent bone morphogenic markers were calculated. As expected, trabecular structure continuously diminished over 12 weeks in OVX compared to Ctrl rats (Figure 1).

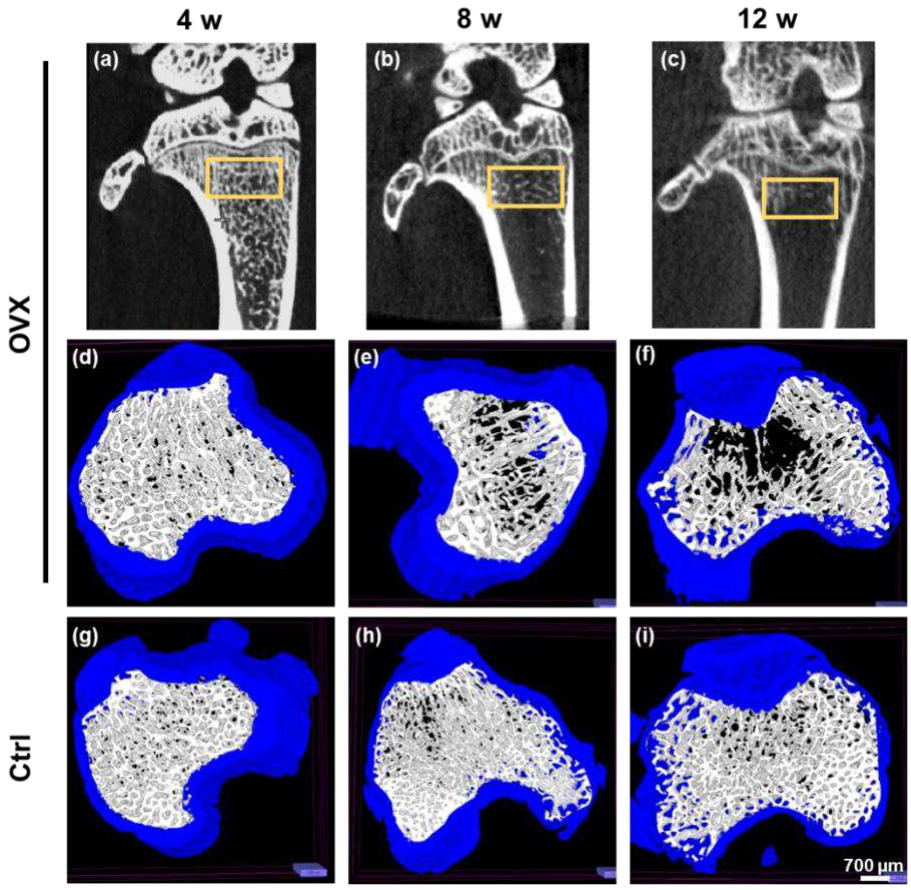

Figure 1: Osteoporosis leads to reduced trabecular bone structure after ovariectomy in female Sprague Dawley rats. *In vivo* low-medium resolution µCT (a) 4, (b) 8 and (c) 12 weeks post-ovariectomy. *Ex vivo* high-resolution µCT highlights the deteriorated trabecular bone structure (d) 4, (e) 8 and especially (f) 12 weeks after ovariectomy compared to control animals (Ctrl; g-i).

Additionally, BV/TV, Tb.Th, Tb.N, Tb.Sp and Conn.D was calculated via CTan and CTVox Software. In line with the observation from the µCT images, we found a significant decrease in BV/TV, Tb.N, and Conn.D as well as a significant increase of Tb.Sp of OVX compared to Ctrl rats, 12 weeks after ovariectomy (Figure 2).

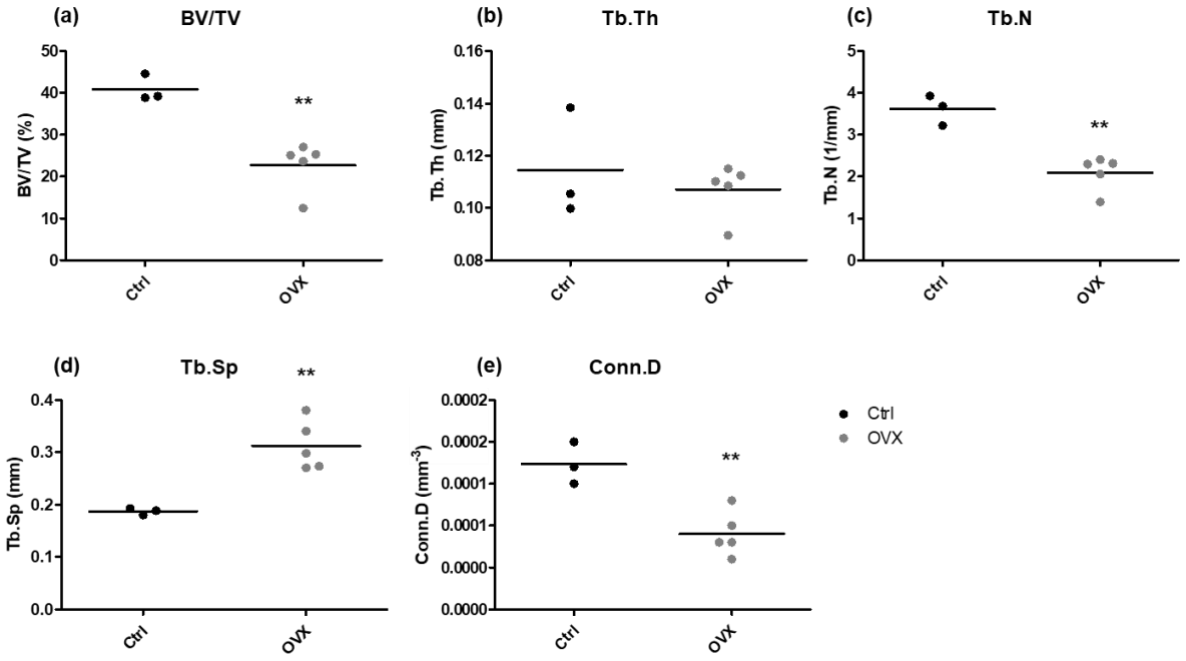

Figure 2: Bone morphometric markers were altered upon ovariectomy 12 weeks after intervention . 3D-reconstructed images underwent quantitative analysis of a) BV/TV, b) Tb.Th, c) Tb.N, d) Tb.Sp and e) Conn.D.

4.2 Flow cytometry 4, 8, 12 weeks

Unfortunately, 4 weeks after ovariectomy, cell isolation did not work. Therefore, we could not obtain flow cytometry results of this group.

Eight weeks after ovariectomy (Figure 3a-c), there was no difference in immune cell populations isolated from blood between the OVX and Ctrl group (Figure 3a). Interestingly, B cell population was significantly decreased in lymph nodes isolated from the OVX compared to Ctrl rats and CD8+ T-cells showed an increased trend in OVX versus Ctrl rats, respectively (Figure 3b). Moreover, $CD8^+$ T-cells were significantly increased in spleen isolated from the OVX compared to the Ctrl group (Figure 3c).

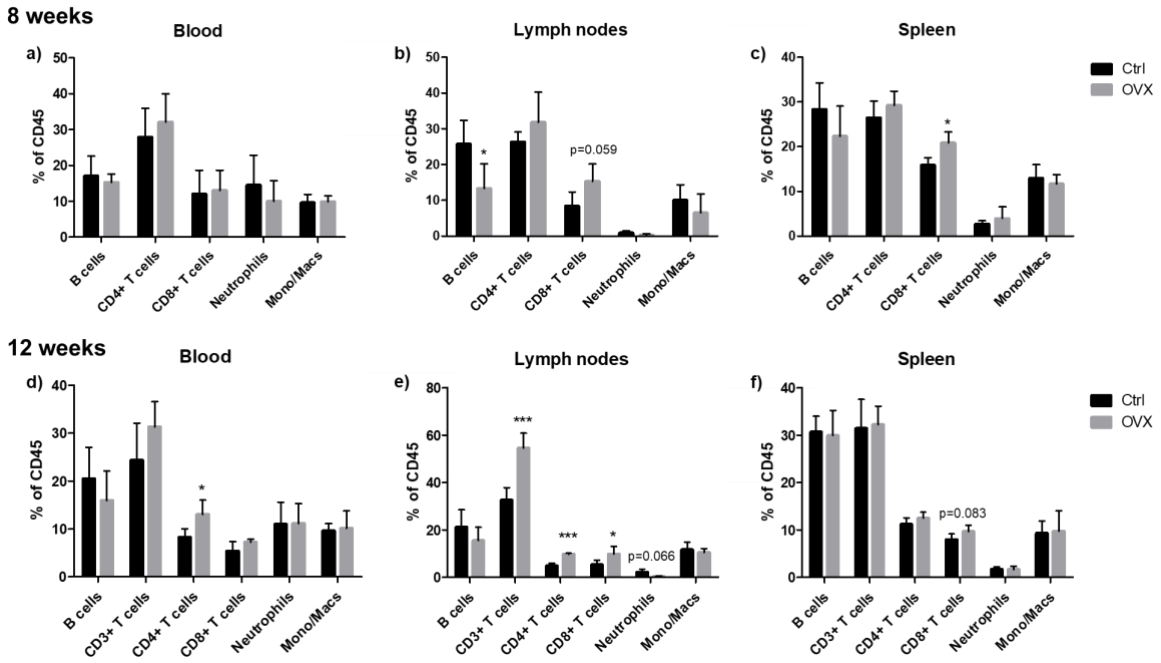

Figure 3: Quantitative analysis of immune cell population in percentage per CD45. Blood was drawn and lymph nodes and spleen were excised from OVX and Ctrl rats a-c) 8 and d-f) 12 weeks after ovariectomy. Results are presented as mean ± standard deviation. Statistical analysis was performed for the particular immune cell population with Student's t-test. *p<0.05, ***p<0.001

Twelve weeks after ovariectomy (Figure 3d-f), $CD4^+$ T-cells were significantly increased in blood, isolated from OVX compared to Ctrl animals (Figure 3d). In lymph nodes, total $CD3^+$ T-cells as well as the $CD4^+$ and $CD8^+$ sub-populations were significantly higher in OVX than Ctrl rats. Moreover, neutrophils isolated from OVX rats showed a marked trend in decrease (Figure 3e, p=0.066) when compared to Ctrl rats. There was no significant difference in immune cell population in spleen cells between the OVX and Ctrl groups. However, $CD8^+$ T-cells showed an increased trend in OVX compared to Ctrl rats (Figure 3f).

4.3 Hard tissue histology

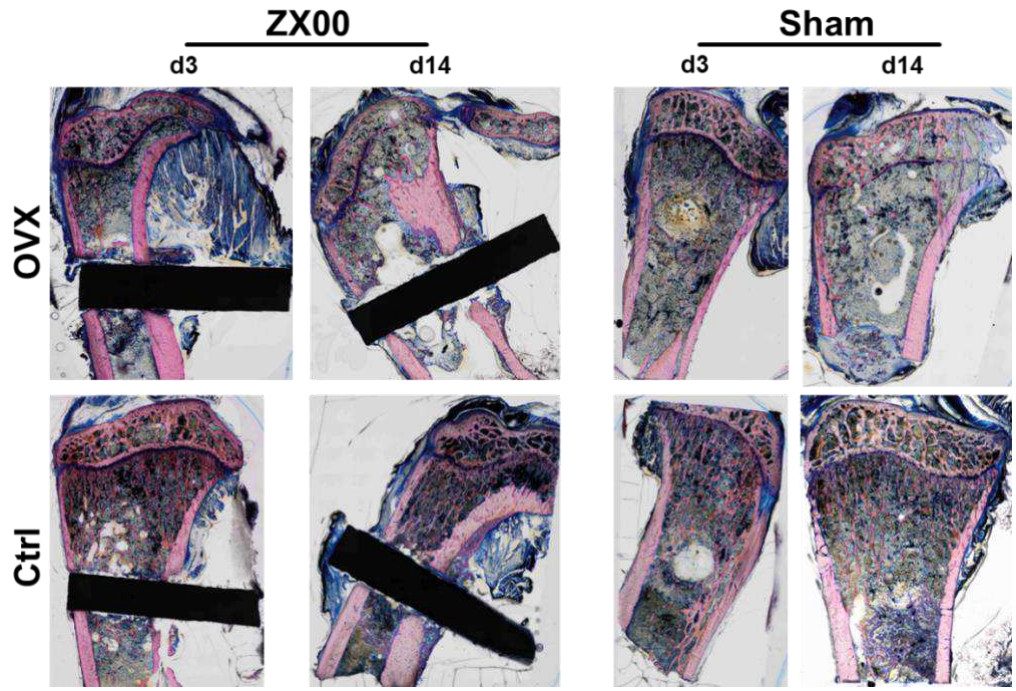

Figure 4: Histological staining after Levai-Laczko, 3 and 14 days post-implantation. *Tibiae were excised, embedded in Technovit 9100 New and 100 µm thin-ground sections were stained after Levai and Laczko.*

Histological observation 3 and 14 days post-surgery confirmed preliminary data suggesting accelerated implant degradation in OVX compared to Ctrl rats. Moreover, qualitative analysis of sham-operated bones indicated more pronounced bone formation in Ctrl compared to OVX rats, supporting the slow healing capacity of bone under osteoporotic conditions.

4.4 Flow cytometry after ZX00 implantation or sham surgery

At the time point of 3 days, the percentage of T cells was almost identical across all four groups in the lymph node samples, with a slight reduction observed in the nOVX (non-ovariectomized rats = Ctrl) ZX00 group. After 14 days, the OVX groups demonstrated an increased proportion of T cells, whereas the nOVX groups exhibited a decrease. The difference between OVX ZX00 and nOVX ZX00 at 14 days was highly significant. The sham groups at this time point displayed a similar trend, although the difference was less

significant (Figure 5a). To achieve better differentiation, T cells were subdivided into CD4-positive and CD8-positive subsets. The results for CD+ T cells revealed a pattern similar to that observed in the overall T cell population, but with numerous highly significant differences. These differences include a decrease in the groups nOVX ZX00 from time point 3 days to time point 14 days, and nOVX sham from time point 3 days to time point 14 days.

Additionally, OVX ZX00 after 14 days exhibited a significantly higher percentage of CD4-positive T cells compared to nOVX ZX00, as well as OVX sham compared to nOVX sham (Figure 5b).

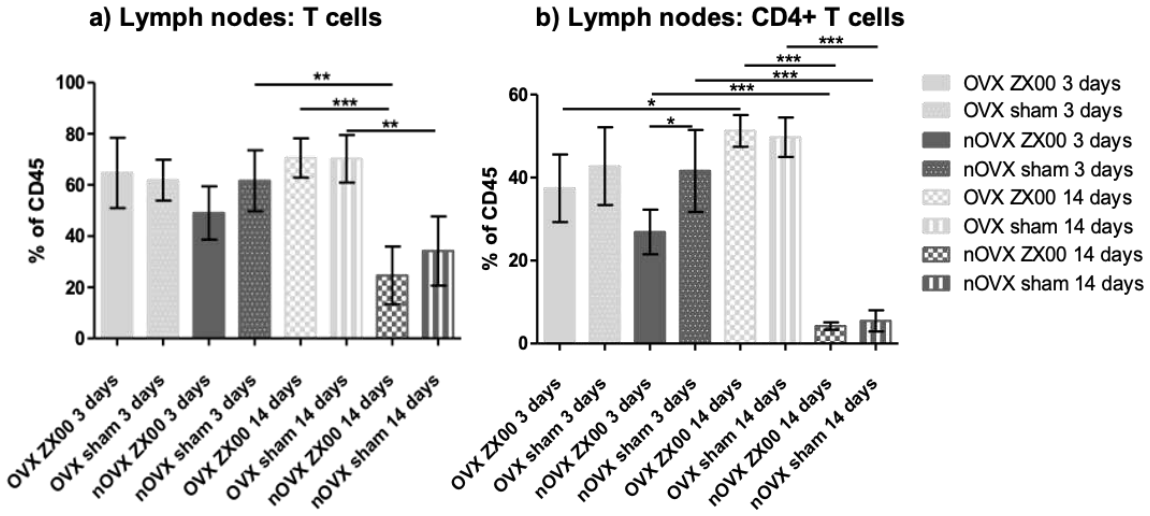

Figure 5: Percentage of total **T cells and CD4+ T cells among CD45-positive immune cells in lymph node samples, at time points 3d and 14d.** a) total T cells b) CD4+ T cells. Results are presented as mean ± SD. Statistical analysis was performed for the particular immune cell population with one-way ANOVA. *p<0.05, **p<0.01, ***p<0.001

The results for CD8-positive T cells indicated a significant decrease between the groups nOVX ZX00 3 and 14 days (Figure 6a).

In regard of B cells, we did not observe any significant difference between all groups (Figure 6b).

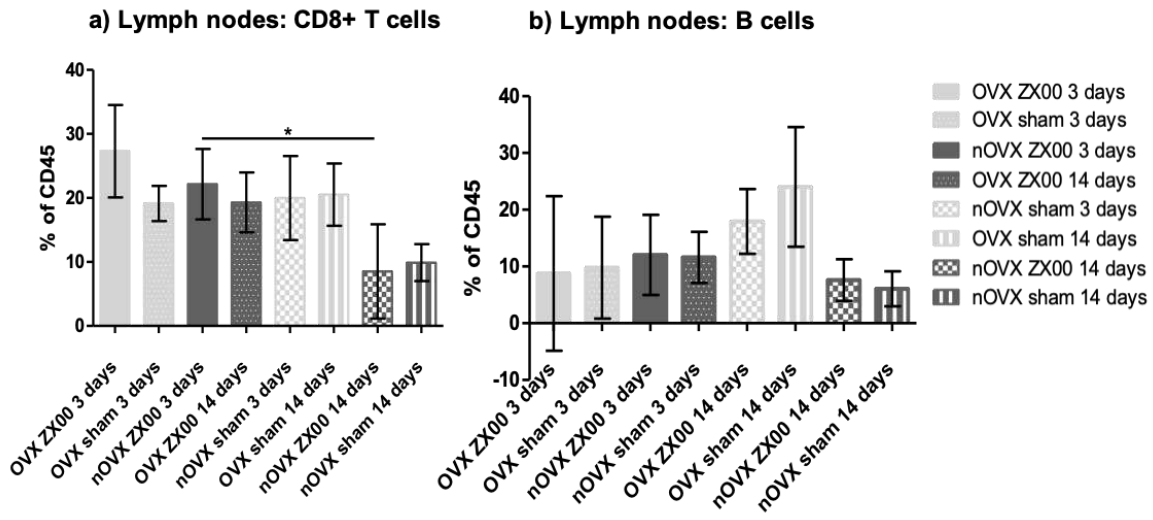

Figure 6: Percentage of CD8+ T cells and B cells among CD45-positive immune cells in lymph node samples, at time points 3d and 14d. a) CD8+ T cells b) B cells. Results are presented as mean ± SD. Statistical analysis was performed for the particular immune cell population with one-way ANOVA. *p<0.05.

In granulocytes, significant increases were observed in the nOVX ZX00 group at 14 days compared to the nOVX ZX00 group at 3 days and the OVX ZX00 group at 14 days. The proportion of granulocytes approached zero in all groups except for nOVX ZX00 and nOVX sham (Figure 7a).

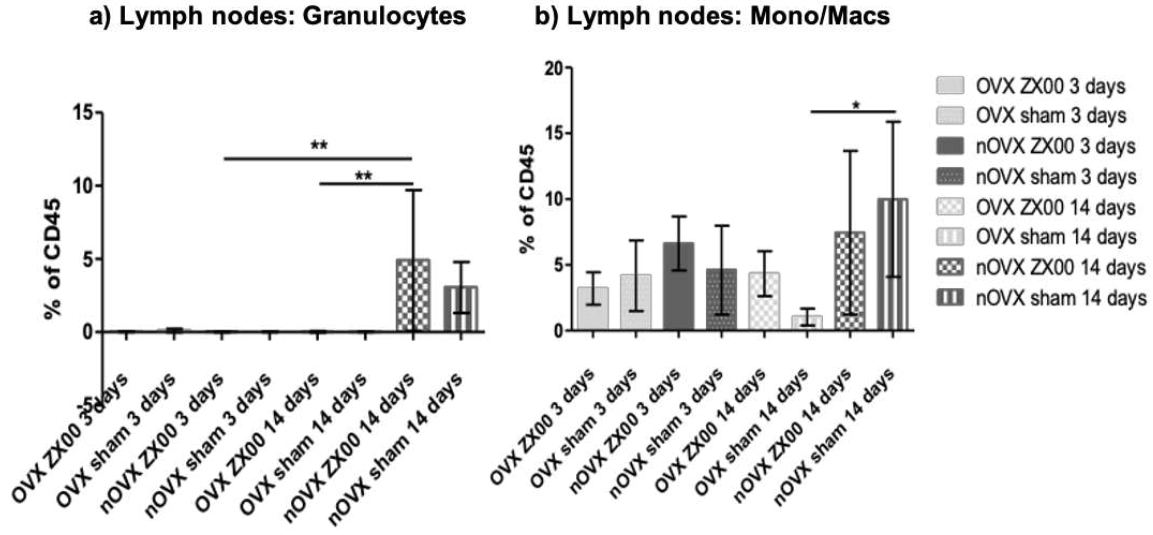

Figure 7: Percentage of Granulocytes and Mono/Macs among CD45-positive immune cells in lymph node samples, at time points 3d and 14d. a) Granulocytes b) Mono/Macs. Results are presented as mean ± SD. Statistical analysis was performed for the particular immune cell population with one-way ANOVA. *p<0.05, **p<0.01.

FACS-analysis describing the proportion of Mono/Macs revealed no significant differences between the groups on day 3. However, Mono/Macs were significantly elevated in the group nOVX sham 14 days compared to OVX sham 14 days (Figure 7b).

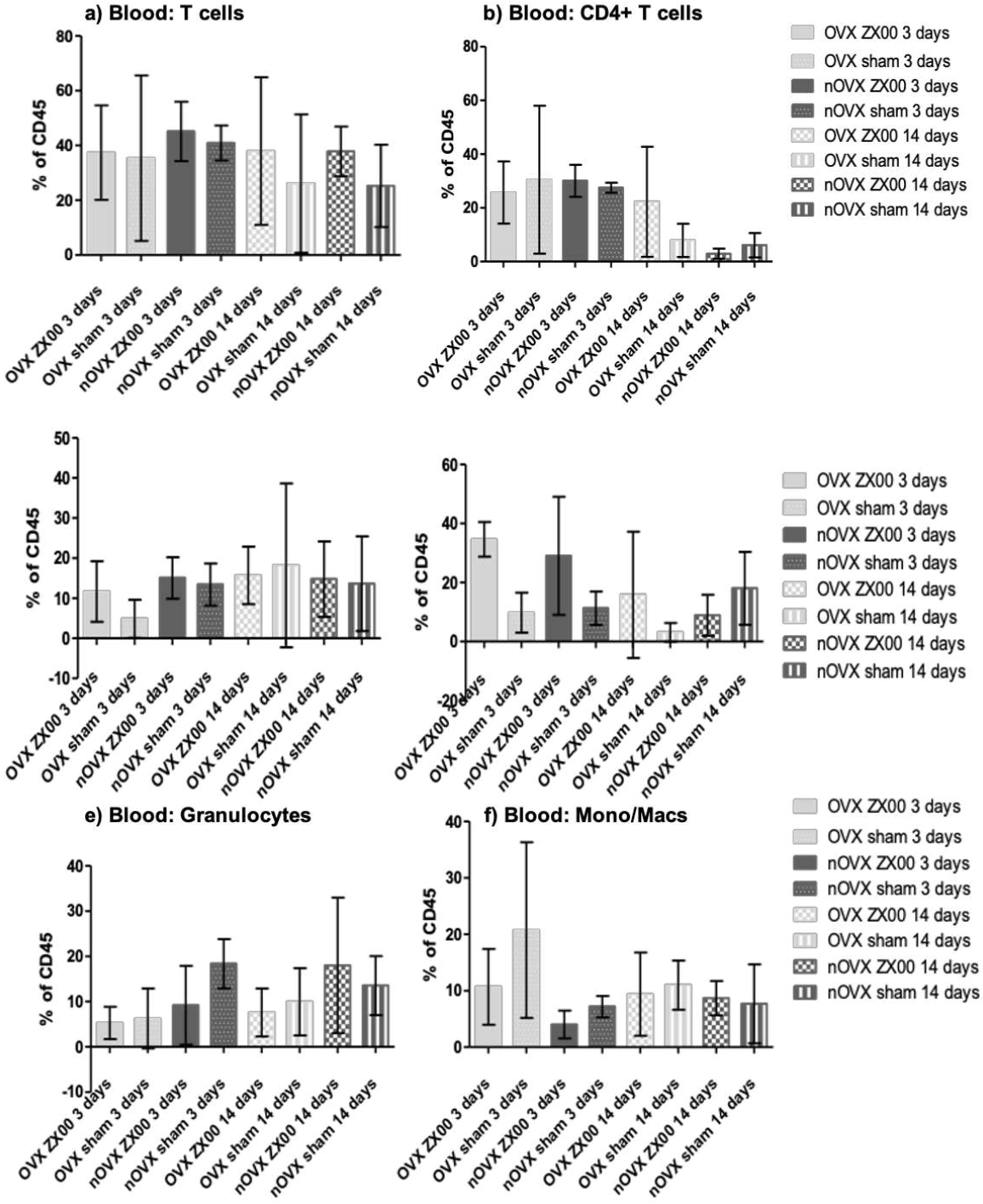

Figure 8: Percentage CD45-positive immune cells in blood samples, subdivided by groups and time points. a) T cells b) CD4+ T cell c) CD8+ T cells d) B cells e) Granulocytes f) Mono/Macs. Results are presented as mean ± SD. Statistical analysis was performed for the particular immune cell population with one-way ANOVA.

We additionally investigated immune cell population in the blood via FACS analyses. Interestingly, we did not observe any differences between all groups at distinct time points or for particular immune cell population(Figure 8 a-f).

The spleen also plays a key role in the immune system of individuals. Here we observed that the percentage of T cells was almost identical across all four groups at time point 3 days, similarly to the lymph node samples. At the 14-day time point, the proportion of T cells in the OVX ZX00 and OVX sham groups showed a significant increase compared to their nOVX counterparts at the same time point. Besides, the OVX sham 14 days was highly elevated compared to the group after 3 days (Figure 9a).
In further segmentation into CD4+ and CD8-positive T cells, the results for CD4-positive T cells were notably distinguished. At time point 14 days, OVX groups were even more elevated compared to their nOVX counterparts. Furthermore exhibited nOVX groups from 3 days to 14 days a decrease of high significance. OVX ZX00 and OVX sham increased in percentage of CD4+ T cells from 3 days to 14 days, even though the change was of lower significance (Figure 9b).

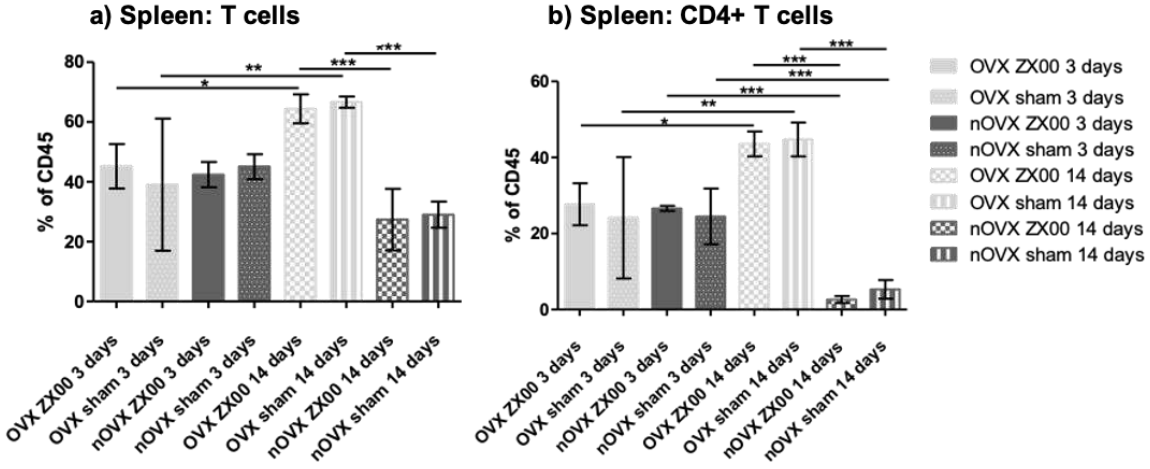

Figure 9: Percentage of total T cells and CD4+ T cells among CD45-positive immune cells in spleen samples, at time points 3d and 14d. a) total T cells b) CD4+ T cells. Results are presented as mean ± SD. Statistical analysis was performed for the particular immune cell population with one-way ANOVA. *p<0.05, **p<0.01, ***p<0.001

In the subset of CD8+ T cells showed no divergencies to point out. All groups ranged between 15% to 25% CD8-positive T cells (Figure 10a).

The results for B cells showed a significantly higher percentage in nOVX ZX00 compared to OVX ZX00 at time pint 3 days. The group nOVX sham decreased from 3 days to 14 days (Figure 10b).

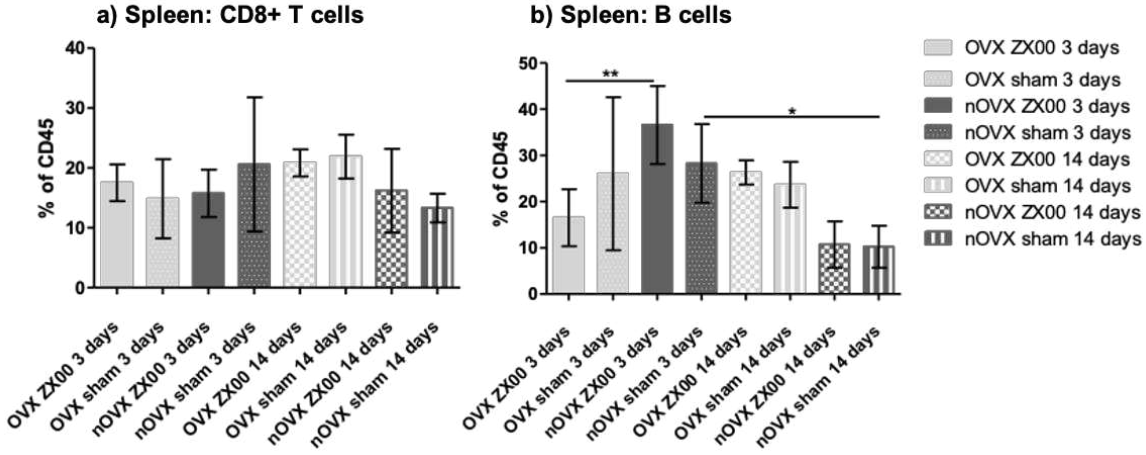

Figure 10: Percentage of CD8+ T cells and B cells among CD45-positive immune cells in spleen samples, at time points 3d and 14d. a) CD8+ T cells b) B cells. Results are presented as mean ± SD. Statistical analysis was performed for the particular immune cell population with one-way ANOVA. *p<0.05, **p<0.01.

In granulocytes the biggest change appeared in the nOVX ZX00 group from 3 days to 14 days with a highly significant increase. At the timepoint 14 days, nOVX ZX00 was significantly elevated compared to OVX ZX00 as well as nOVX sham to OVX sham (Figure 11a).

In the subdivision of Mono/macs, the proportions in the nOVX ZX00 and nOVX sham groups at the 14-day time point were significantly elevated compared to their OVX counterparts. Additionally, at this time point, the nOVX sham group was also significantly elevated compared to the nOVX sham group at the 3-day time point. A similar pattern was observed in the nOVX ZX00 group, where the proportion at 14 days was significantly elevated compared to the nOVX ZX00 group at 3 days (Figure 11b).

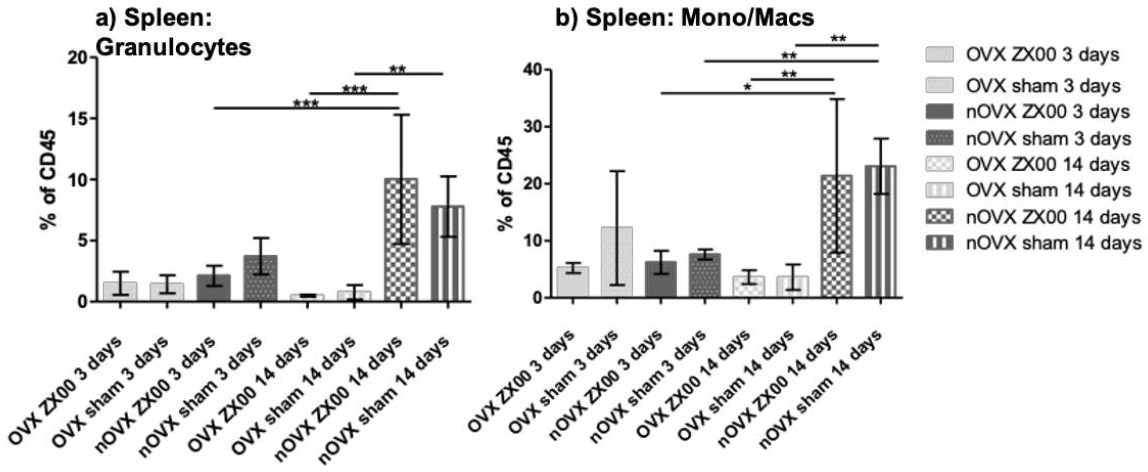

p

Figure 11: Percentage of Granulocytes and Mono/Macs among CD45-positive immune cells in spleen samples, at time points 3d and 14d. a) Granulocytes b) Mono/Macs. Results are presented as mean ± SD. Statistical analysis was performed for the particular immune cell population with one-way ANOVA. *p<0.05, **p<0.01, ***p<0.001

5 Discussion

Demographic change is trending toward an aging society. Hence, there is rising prevalence of postmenopausal and senile osteoporosis (1). Postmenopausal osteoporosis is related to estrogen deficiency and characterized by increased osteoclast activity (113), whereas senile osteoporosis predominantly develops due to aging and is characterized by decreased osteoblast activity and increased reactive oxygen species, impaired DNA repair and vitamin D deficiency (114). Pharmacotherapy with bisphosphonates and SERMs appears to be effective but is limited by wearing-off and underdiagnosis of the disease itself. Consequently, the number of osteoporotic fractures is rising. Due to prolonged disease courses with high treatment costs, this becomes not only a health issue, but also an economic problem (1, 10, 18).

The osteosynthesis of osteoporotic-related fragility fractures is associated with several challenges: the bone healing capacity is reduced, which limits the implant anchorage due to decreased bone mineral density. Additionally, osteoporotic bone has a lower tolerance for implant side effects, such as stress shielding and toxicity of degradation particles (115). Accordingly, the demands on osteoconductivity, osteoinductivity, and the e-modulus are higher compared to healthy bone. Ti alloys, high-grade steel, and synthetic polymers are predominantly used to stabilize bone fractures. These materials insufficiently meet the requirements pinpointing to the high demand for innovative implant materials. In this context, Mg-based implants have gained significant attention. The properties were significantly improved in terms of corrosion behavior and biocompatibility by alloying and surface modulation (47, 116). For instance, Okutan et al. demonstrated favorable properties of Mg alloyed with Zn and Ca, designated as ZX00, when compared to ultrahigh-purity Mg (117). Although numerous studies examined ZX00, the majority was limited to research in healthy bone (118-121). Sommer et al. demonstrated increased ZX00 implant degradation with massive gas evolution in osteoporotic rats compared to old and juvenile healthy animals (112), indicating to a disease-related effect that enhances ZX00 degradation. Consequently, it is essential to investigate the interaction between implant materials and bone, as well as the immune response, under osteoporotic conditions. In the first part of our study, we ovariectomized 15 Sprague-Dawley rats at the

age of 9 months. *In vivo* low to medium resolution and *ex vivo* high-resolution µCT was performed at the timepoints 4, 8, and 12 weeks. The progression of osteoporosis was evident in the *in vivo* µCT images obtained at various time points. At 12 weeks, the OVX group exhibited a notably reduced trabecular bone structure compared to the Ctrl group. The bone morphometric markers 12 weeks after ovariectomy showed a concordant result to the µCT images. Previously, Sommer et al. showed the ovariectomy-induced osteoporosis progression in *in vivo* µCT for a period of 4, 8, and 12 weeks in rats that were ovariectomized at the age of 12 months. The result displayed a significant loss of trabecular density, especially after 12 weeks (112). The difference of the rats' age at the time point of ovariectomy is 12 months in the study by Sommer et al., compared to 9 months in this study. This difference has only a marginal impact on the results, as the skeletal maturation of rats is achieved between 3 to 6 months for cancellous bone and 9 to 12 months for cortical bone, with peak bone mass being reached at 10 months (122, 123). As expected, our results were concordant, which was also supported by the *ex vivo* images pinpointing to progressive loss of trabecular density.

The calculated bone morphometric parameters, including bone volume fraction (BV/TV), trabecular number (Tb.N), and connectivity density (Conn.D), were significantly decreased in the OVX group compared to the control group, whereas trabecular separation (Tb.Sp) showed a significant increase. The concept of utilizing µCT imaging and bone morphometric parameters to display the development of osteoporosis in rodents for preclinical research is well-established and widely applied in many studies (124). Boyd et al. utilized µCT imaging and bone morphometric parameters to establish the normal time course of bone loss in OVX rats over a period of 6 months after ovariectomy (125). In another study, the rapid development of osteoporosis in OVX rats with a low-calcium diet, compared to sham rats and OVX rats, was demonstrated by an increase in Tb.Sp and a decrease in Tb.Th and Tb.N (126). Although these outcomes were anticipated, given that ovariectomized rats are a well-established model for simulating postmenopausal osteoporosis, confirmation was essential to examine the systemic immune response to Mg-based implants (ZX00) and to assess implant integration under both, osteoporotic and healthy conditions. Additionally, lymph node, spleen, and blood samples were excised at each sacrification time point to quantitatively analyze the immune cell population in percentage per CD45 using flow cytometry. After 8 weeks, B cells were

significantly lower in the lymph nodes of the OVX compared to the Ctrl group, whereas CD8+ T cells were significantly elevated in OVX compared to Ctrl. Twelve weeks post-ovariectomy, CD4+ T-cells were significantly elevated in the blood of OVX compared to Ctrl animals. In lymph nodes, total CD3+ T-cells, along with CD4+ and CD8+ sub-populations, were significantly higher in OVX rats. No significant differences in immune cell populations were observed in spleen cells, although CD8+ T-cells showed an increasing trend in OVX rats. The increase in T cell levels observed during the progression was expected, as multiple studies in humans and rodents have demonstrated a link between the rise in T cells and estrogen deficiency-induced osteoporosis (127, 128). Srivastava et al. highlighted the pivotal role of T cells in the pathogenesis of inflammatory bone disorders, such as osteoporosis, and identified these cells as potential therapeutic targets (90).

After 8 weeks, a significant decrease in B cell levels was observed in the lymph nodes of OVX subjects compared to the Ctrl group. The significant difference in B cells did not progress over the period from 8 to twelve weeks. On the contrary, the B cell numbers converged in all specimens. This observation is consistent with studies that report an increase in B cell populations during the progression of estrogen deficiency-induced osteoporosis (129). However, other studies in mice and humans have indicated a decrease in B cell numbers, highlighting the complexity and variability of their role in this condition (91, 130). Although the involvement of B cells in estrogen deficiency-induced osteoporosis is considered well-established, their precise role remains incompletely understood (98, 130).

Here we demonstrated that the immunological evidence supports the development of osteoporosis highlighted by bone alterations. In brief, we successfully visualized the bone morphological changes associated with the onset of osteoporosis using *in vivo* and *ex vivo* µCT imaging, complemented by bone morphometric markers derived from 3D reconstructions. The results of the quantitative analysis of immune cell populations showed a clear inflammatory state.

Next, we randomly divided 40 Sprague-Dawley rats into four groups: OVX ZX00, nOVX(Ctrl) ZX00, OVX sham, and nOVX(Ctrl) sham. Animals were sacrificed at 3 and 14 days post implantation.

We qualitatively observed reduced bone formation in the OVX-sham group compared to the nOVX(Ctrl) sham group. In a systematic review by Chen et al. reduced bone healing in fractures of ovariectomized rats was demonstrated (131). Chen et al. compared 25 studies with fracture models in ovariectomized rats (131). Although the results are in line with our study, it is notable that a fracture model is not completely comparable to the sub-critical size defect in our study. He et al. have demonstrated reduced bone healing of sub-critical size defects in ovariectomized mice with drill holes created in the femur (132). Despite differences in defects or animal species the results are in accordance with Chen et al. and He et al. Study designs using ovariectomized rats are well-established for investigating metaphyseal fractures in osteoporotic bone, particularly in relation to decreased healing (e.g., Wong et al. (133)). Furthermore, the OVX group showed an increased implant degradation compared to the nOVX(Ctrl) group. Only previously, Sommer et al. showed accelerated degradation of ZX00 implants in osteoporotic rats compared to old healthy and juvenile healthy rats (112). Interestingly, Zhang et al. revealed the promoting effect of implant-derived Mg^{2+} ions on CGRP production in osteoporotic rats, thereby improving fracture healing by enhancing osteogenesis (134). Further studies addressed the impact of Mg-incorporated implant coating. Galli et al. demonstrated the beneficial influence of Mg^{2+} released from Mg coated Ti screws to the early phase of osseointegration in osteoporotic rats (135). Li et al. compared Mg-incorporated hydroxyapatite (MgHA) coating with HA coating on Ti implants in OVX rats and described an enhancing effect of Mg-incorporated coatings on osseointegration as well (136). With exception of Sommer et al., all authors primarily focused on the effect of Mg on the osteoporotic bone and bone-implant interface. Limited attention has been given to the possibility that the inflammatory process of osteoporosis might also affect implant's behavior.

Here, FACS analysis displayed major changes in T cells, which were primarily driven by CD4+ T cells. CD4+ T cells showed an initial increase in response to surgical trauma across all groups compared to results obtained 12 weeks post-ovariectomy, in both lymph nodes and spleen. An increase in CD4+ T cells in lymph nodes and spleen following trauma was also demonstrated by Yamakawa et al. in a mouse study with flow cytometry (137). Interestingly, ZX00 reduced the initial CD4+ response in the lymph nodes, even

significantly in the nOVX(Ctrl) group. The lymph nodes were harvested from the inguinal region, which is in closer anatomical proximity to the surgical site than the spleen. Thus, local immunomodulation by released Mg^{2+} might be less diluted and consequently more pronounced in the FACS analysis. Peng et al. demonstrated in mice with Mg-coated Ti implants a locally increased M2 polarization of macrophages, accompanied by elevated levels of the anti-inflammatory cytokines IL-10 and IL-4, as well as reduced levels of the pro-inflammatory cytokines TNF-α, IL-1β, and IL-6 (138). Il-6 has been shown to be a major driver for CD4+ T cell expansion, as Nish et al. demonstrated in mice with IL-6Rα deficient T cells (139). The initial differences in CD4+ T cells between the ZX00 and sham groups were no longer observed in the spleen or lymph nodes after 14 days. The significant increase in CD4+ T cell population might be related to ovariectomy, since nOVX(Ctrl) groups' CD4+ T cell levels significantly declined. This aligns with findings of Shao et al., who demonstrated elevated CD4+ T cell levels in flow cytometry analysis of the spleen in mice 8 weeks post-ovariectomy (140). Interestingly, at 3 days post-surgery (sham or ZX00) B cell levels decreased about 50% in spleen of OVX animals with ZX00 pins, whereas nOVX(Ctrl) groups showed a slight increase when compared to baseline levels measured at 12 weeks in OVX and nOVX(Ctrl) animals. This suggests that Mg may reduce the systemic B cell response in osteoporotic condition. To the best of our knowledge there are no studies investigating the systemic immune response of Mg-based implants, especially in osteoporotic conditions.

However, the cells of the innate immune system showed a more pronounced increase in the healthy condition. For instance, results indicated enhanced granulocyte response after 14 days in both, lymph nodes and spleen, of healthy rats. . As mentioned earlier, there is a lack of studies investigating the systemic immune response to Mg-based implants in tissues like lymph nodes and spleen. Although the local reaction may not be directly transferable to the systemic level, it can be considered an interesting perspective for potential future studies. For example, Riyaz et al. investigated the immune response to Mg and Mg-10Gd implants *in vivo* using a rat femur fracture model. The study employed fluorescence molecular tomography (FMT) for inflammation imaging and flow cytometry to analyze T cell, B cell, and neutrophil populations around the implant. The findings revealed no significant increase in inflammation around the Mg and Mg-10Gd implants; however, there was a notable increase in neutrophils in the Mg group 28 days post-

implantation (141). Accordingly, local effects around Mg-based implants might be affected in osteoporotic condition. Since we also observed an increase in neutrophils in the spleen and lymph nodes, future studies investigating neutrophils' role under osteoporotic conditions are warranted. However, some studies investigated changes in blood samples. Castellani et al. compared biodegradable Mg implants to Ti implants in a rat model and analyzed granulocyte levels in the blood at 4, 12, and 24 weeks post-implantation (142). No significant changes were observed in any of these parameters. Similarly, Zhang et al. evaluated the effects of biodegradable Mg alloy bone implants during the first 6 months after implantation and found no relevant changes in red blood cell count, platelet count, or white blood cell count in the period from 6 to 26 weeks (143). The findings of both studies align with this study, although there is a difference in time points.

Taken together, this study demonstrated that Mg released from implants can modulate the systemic immune response to surgery and implantation in osteoporotic bone, although just marginally, particularly during the first days. Differences between osteoporotic and healthy bone were evident, even over time. The major changes in the immune response appeared to be primarily due to the ovariectomy, regardless of ZX00 implants or sham surgery. A longer observation period may be beneficial to evaluate the potential for long-term modulation by released Mg^{2+} ions. Importantly, the systemic immune response was assessed using samples from the spleen, lymph nodes, and blood. However, the local immune response might differ. This is suggested by the fact that results from the three tissue types varied, and in some cases, even contradicted one another.

Limitations

A notable limitation is the unsuccessful cell extraction from the 4-week specimens for FACS analysis. Including a third time point could have provided better contextualization of B cell changes, and extending the observation period may have offered additional insights. Furthermore, a direct comparison of systemic and local reactions within a single study could be useful.

6 Conclusion

In summary, this study successfully demonstrated the implementation of an animal model using osteoporotic rats. The development of osteoporosis was confirmed through FACS analysis at the level of systemic immune response, as well as µCT imaging and bone morphometric markers. On this basis of this rat study the increased degradation of the ZX00 was shown in osteoporotic bone. The released Mg^{2+} ions marginally modulate the systemic reaction. In osteoporotic bone, differences to surgery were primarily observed in the early stage of inflammation. Over a longer observation period, this effect appears to diminish indicating the transition of acute to intermediate pro-inflammatory reaction. Further studies focusing on local changes in immune cells in response to Mg-based implants and a longer observation period would be valuable. This allows for a weighing of the benefits of the positive immunomodulatory effects of Mg against the potential negative aspects of faster implant degradation.

Reference list

1. Kanis JA, Norton N, Harvey NC, Jacobson T, Johansson H, Lorentzon M, et al. SCOPE 2021: a new scorecard for osteoporosis in Europe. Arch Osteoporos. 2021;16(1):82.
2. Eriksen EF, Hodgson SF, Eastell R, Cedel SL, O'Fallon WM, Riggs BL. Cancellous bone remodeling in type I (postmenopausal) osteoporosis: quantitative assessment of rates of formation, resorption, and bone loss at tissue and cellular levels. J Bone Miner Res. 1990;5(4):311-9.
3. Parfitt AM, Villanueva AR, Foldes J, Rao DS. Relations between histologic indices of bone formation: implications for the pathogenesis of spinal osteoporosis. J Bone Miner Res. 1995;10(3):466-73.
4. Emkey GR, Epstein S. Secondary osteoporosis: Pathophysiology & diagnosis. Best Practice & Research Clinical Endocrinology & Metabolism. 2014;28(6):911-35.
5. Kiernan J, Davies JE, Stanford WL. Concise Review: Musculoskeletal Stem Cells to Treat Age-Related Osteoporosis. Stem Cells Translational Medicine. 2017;6(10):1930-9.
6. Tella SH, Gallagher JC. Bazedoxifene + conjugated estrogens in HT for the prevention of osteoporosis and treatment of vasomotor symptoms associated with the menopause. Expert Opin Pharmacother. 2013;14(17):2407-20.
7. Kanis J, Glüer C. International Osteoporosis Foundation. An update on the diagnosis and assessment of osteoporosis with densitometry. Osteoporos Int. 2000;11(3):192-202.
8. Kanis JA, Kanis JA. Assessment of fracture risk and its application to screening for postmenopausal osteoporosis: Synopsis of a WHO report. Osteoporosis International. 1994;4(6):368-81.
9. Kanis JA, McCloskey EV, Johansson H, Oden A, Melton LJ, Khaltaev N. A reference standard for the description of osteoporosis. Bone. 2008;42(3):467-75.
10. Prophylaxe, Diagnostik und Therapie der Osteoporose bei postmenopausalen Frauen und bei Männern - Leitlinie der DVO. 2023.

11. Schini M, Johansson H, Harvey NC, Lorentzon M, Kanis JA, McCloskey EV. An overview of the use of the fracture risk assessment tool (FRAX) in osteoporosis. Journal of Endocrinological Investigation. 2024;47(3):501-11.
12. Langdahl BL. Overview of treatment approaches to osteoporosis. Br J Pharmacol. 2021;178(9):1891-906.
13. Graefe K-H. Pharmakologie und Toxikologie. 2., vollständig überarbeitete Auflage ed. Stuttgart: Thieme; 2016.
14. Dar HY, Azam Z, Anupam R, Mondal RK, Srivastava RK. Osteoimmunology: The Nexus between bone and immune system. Front Biosci (Landmark Ed). 2018;23(3):464-92.
15. Srivastava RK, Sapra L. The Rising Era of "Immunoporosis": Role of Immune System in the Pathophysiology of Osteoporosis. J Inflamm Res. 2022;15:1667-98.
16. Gennari L, Merlotti D, Falchetti A, Eller Vainicher C, Cosso R, Chiodini I. Emerging therapeutic targets for osteoporosis. Expert Opin Ther Targets. 2020;24(2):115-30.
17. Sung-Jin Kim SJM, J. Seo. Biological characteristics of osteoporosis drugs: the effect of osteoblast–osteoclast coupling. International Journal of Oral Biology. 2019.
18. Miller PD. Underdiagnosis and Undertreatment of Osteoporosis: The Battle to Be Won. J Clin Endocrinol Metab. 2016;101(3):852-9.
19. Ficklscherer A-. Kurzlehrbuch Orthopädie und Unfallchirurgie. 2., komplett überarbeitete und aktualisierte Auflage ed2024.
20. Niethard F. U. BP. Duale Reihe Orthopädie und Unfallchirurgie Thieme; 2022.
21. Bühren V. KM, Marzi I. Checkliste Traumatologie Thieme; 2016.
22. Orthopädie und Unfallchirurgie Facharztwissen nach der neuen Weiterbildungsordnung. 1. Aufl. ed. Scharf H-P, editor. München Jena: Urban & Fischer in Elsevier; 2009.
23. Albrektsson T, Johansson C. Osteoinduction, osteoconduction and osseointegration. Eur Spine J. 2001;10 Suppl 2:S96-101.
24. Shekhawat DS, A.; Bhardwaj, A.; Patnaik, A. A Short Review on Polymer, Metal and Ceramic Based
Implant Materials. IOP Conf Ser Mater Sci Eng. 2021.

25. Overmann AL, Aparicio C, Richards JT, Mutreja I, Fischer NG, Wade SM, et al. Orthopaedic osseointegration: Implantology and future directions. J Orthop Res. 2020;38(7):1445-54.
26. Chen Q. TGA. Metallic implant biomaterials. Materials Science and Engineering: R: Reports. 2015;87.
27. Szczesny G, Kopec M, Politis DJ, Kowalewski ZL, Lazarski A, Szolc T. A Review on Biomaterials for Orthopaedic Surgery and Traumatology: From Past to Present. Materials (Basel). 2022;15(10).
28. Witte F, Kaese V, Haferkamp H, Switzer E, Meyer-Lindenberg A, Wirth CJ, et al. *In vivo* corrosion of four magnesium alloys and the associated bone response. Biomaterials. 2005;26(17):3557-63.
29. Aherwar A. PA. Cobalt based alloy: A better choice biomaterial for hip implants. Trends in Biomaterials and Artificial Organs. 2016.
30. R.P. V. Titanium based biomaterial for bone implants: A mini review. materialstoday:PROCEEDINGS. 2020;26.
31. Nasibi SA, K.; Bazli, L.; Eskandarinezhad, S.; Mohammadi, A.; Sheysi, N. TZNT alloy for surgical implant applications: A Systematic Review. J Compos Compd. 2020.
32. Le Guéhennec L, Soueidan A, Layrolle P, Amouriq Y. Surface treatments of titanium dental implants for rapid osseointegration. Dental materials. 2007;23(7):844-54.
33. Alghamdi HS, Junker R, Bronkhorst EM, Jansen JA. Bone regeneration related to calcium phosphate-coated implants in osteoporotic animal models: a meta-analysis. Tissue Engineering Part B: Reviews. 2012;18(5):383-95.
34. Reith G, Schmitz-Greven V, Hensel KO, Schneider MM, Tinschmann T, Bouillon B, et al. Metal implant removal: benefits and drawbacks–a patient survey. BMC surgery. 2015;15:1-8.
35. Cheung W.H. MT, Chow S.K., Yang F.F., Alt V. Fracture healing in osteoporotic bone. Injury. 2016;47.
36. Reddy MSB, Ponnamma D, Choudhary R, Sadasivuni KK. A Comparative Review of Natural and Synthetic Biopolymer Composite Scaffolds. Polymers. 2021;13(7):1105.
37. Alizadeh-Osgouei M, Li Y, Wen C. A comprehensive review of biodegradable synthetic polymer-ceramic composites and their manufacture for biomedical applications. Bioactive Materials. 2019;4:22-36.

38. Al-Shalawi FD, Azmah Hanim MA, Ariffin MKA, Looi Seng Kim C, Brabazon D, Calin R, et al. Biodegradable synthetic polymer in orthopaedic application: A review. Materials Today: Proceedings. 2023;74:540-6.
39. Liu H, Slamovich EB, Webster TJ. Less harmful acidic degradation of poly (lactic-co-glycolic acid) bone tissue engineering scaffolds through titania nanoparticle addition. International journal of nanomedicine. 2006;1(4):541-5.
40. Huse EC. A new ligature. The Chicago Medical Journal and Examiner. 1878;37(2):171.
41. Payr E. Beitrage zur Technik der Blutgesfass und Nervennaht nebst Mittheilungen die Verwendung eines Resorbierharen Metalles in der Chirurgie. Arch Klin Chir. 1900;62:67-71.
42. Witte F. The history of biodegradable magnesium implants: a review. Acta Biomater. 2010;6(5):1680-92.
43. Lambotte A. L'utilisation du magnesium comme materiel perdu dans l'osteosynthèse. Bull Mem Soc Nat Chir. 1932;28(3):1325-34.
44. R. Zeng WD, F. Witte, N. Hort, C. Blawert. Progress and Challenge for Magnesium Alloys as Biomaterials. ADVANCED ENGINEERING MATERIALS. 2008;10(8).
45. Wagoner Johnson AJ, Herschler BA. A review of the mechanical behavior of CaP and CaP/polymer composites for applications in bone replacement and repair. Acta Biomaterialia. 2011;7(1):16-30.
46. Uppal G, Thakur A, Chauhan A, Bala S. Magnesium based implants for functional bone tissue regeneration – A review. Journal of Magnesium and Alloys. 2022;10(2):356-86.
47. Witte F, Hort N, Vogt C, Cohen S, Kainer KU, Willumeit R, et al. Degradable biomaterials based on magnesium corrosion. Current Opinion in Solid State and Materials Science. 2008;12(5):63-72.
48. Asgari M, Yang Y, Yang S, Yu Z, Yarlagadda PKDV, Xiao Y, et al. Mg–Phenolic Network Strategy for Enhancing Corrosion Resistance and Osteocompatibility of Degradable Magnesium Alloys. ACS Omega. 2019;4(26):21931-44.
49. Song G. Control of biodegradation of biocompatable magnesium alloys. Corrosion Science. 2007;49(4):1696-701.

50. Staiger MP, Pietak AM, Huadmai J, Dias G. Magnesium and its alloys as orthopedic biomaterials: A review. Biomaterials. 2006;27(9):1728-34.
51. Fischerauer SF, Kraus T, Wu X, Tangl S, Sorantin E, Hänzi AC, et al. *In vivo* degradation performance of micro-arc-oxidized magnesium implants: A micro-CT study in rats. Acta Biomaterialia. 2013;9(2):5411-20.
52. Charyeva O, Feyerabend F, Willumeit R, Szakacs G, Agha N, Hort N, et al. *In vitro* resorption of magnesium materials and its effect on surface and surrounding environment. MOJ Toxicol. 2015;1(1):00004.
53. Myrissa A, Agha NA, Lu Y, Martinelli E, Eichler J, Szakacs G, et al. *In vitro* and *in vivo* comparison of binary Mg alloys and pure Mg. Materials Science and Engineering: C. 2016;61:865-74.
54. Cecchinato F, Agha NA, Martinez-Sanchez AH, Luthringer BJC, Feyerabend F, Jimbo R, et al. Influence of magnesium alloy degradation on undifferentiated human cells. PloS one. 2015;10(11):e0142117.
55. Myrissa A, Braeuer S, Martinelli E, Willumeit-Römer R, Goessler W, Weinberg AM. Gadolinium accumulation in organs of Sprague–Dawley® rats after implantation of a biodegradable magnesium-gadolinium alloy. Acta Biomaterialia. 2017;48:521-9.
56. Amerstorfer F, Fischerauer SF, Fischer L, Eichler J, Draxler J, Zitek A, et al. Long-term *in vivo* degradation behavior and near-implant distribution of resorbed elements for magnesium alloys WZ21 and ZX50. Acta Biomaterialia. 2016;42:440-50.
57. Witte F, Kaese V, Haferkamp H, Switzer E, Meyer-Lindenberg A, Wirth CJ, et al. *In vivo* corrosion of four magnesium alloys and the associated bone response. Biomaterials. 2005;26(17):3557-63.
58. Zhang J, Li H, Wang W, Huang H, Pei J, Qu H, et al. The degradation and transport mechanism of a Mg-Nd-Zn-Zr stent in rabbit common carotid artery: A 20-month study. Acta biomaterialia. 2018;69:372-84.
59. Cihova M, Martinelli E, Schmutz P, Myrissa A, Schäublin R, Weinberg AM, et al. The role of zinc in the biocorrosion behavior of resorbable Mg–Zn–Ca alloys. Acta Biomaterialia. 2019;100:398-414.
60. Holweg P, Berger L, Cihova M, Donohue N, Clement B, Schwarze U, et al. A lean magnesium–zinc–calcium alloy ZX00 used for bone fracture stabilization in a large growing-animal model. Acta Biomaterialia. 2020;113:646-59.

61. Labmayr V, Suljevic O, Sommer NG, Schwarze UY, Marek RL, Brcic I, et al. Mg-Zn-Ca Alloy (ZX00) Screws Are Resorbed at a Mean of 2.5 Years After Medial Malleolar Fracture Fixation: Follow-up of a First-in-humans Application and Insights From a Sheep Model. Clinical Orthopaedics and Related Research®. 2024;482(1):184-97.
62. Herber V, Labmayr V, Sommer NG, Marek R, Wittig U, Leithner A, et al. Can Hardware Removal be Avoided Using Bioresorbable Mg-Zn-Ca Screws After Medial Malleolar Fracture Fixation? Mid-Term Results of a First-In-Human Study. Injury. 2022;53(3):1283-8.
63. Zhai Z, Qu X, Li H, Yang K, Wan P, Tan L, et al. The effect of metallic magnesium degradation products on osteoclast-induced osteolysis and attenuation of NF-κB and NFATc1 signaling. Biomaterials. 2014;35(24):6299-310.
64. El-Rashidy AA, Roether JA, Harhaus L, Kneser U, Boccaccini AR. Regenerating bone with bioactive glass scaffolds: A review of *in vivo* studies in bone defect models. Acta Biomaterialia. 2017;62:1-28.
65. Witte F, Ulrich H, Palm C, Willbold E. Biodegradable magnesium scaffolds: Part II: Peri-implant bone remodeling. Journal of biomedical materials research Part A. 2007;81(3):757-65.
66. Patrycja L, Julia M, Wojciech N, Sara C, Jeanette AM, Andrzej M. Extracellular Mg concentration and Ca blockers modulate the initial steps of the response of Th2 lymphocytes in co-culture with macrophages and dendritic cells. European Cytokine Network. 2015;26(1):1-9.
67. Zhang X, Chen Q, Mao X. Magnesium Enhances Osteogenesis of BMSCs by Tuning Osteoimmunomodulation. BioMed Research International. 2019;2019(1):7908205.
68. Jin L, Wu J, Yuan G, Chen T. *In vitro* study of the inflammatory cells response to biodegradable Mg-based alloy extract. PLoS One. 2018;13(3):e0193276.
69. Chu W, Li T, Jia G, Chang Y, Liu Z, Pei J, et al. Exposure to high levels of magnesium disrupts bone mineralization *in vitro* and *in vivo*. Ann Transl Med. 2020;8(21):1419.
70. Yu Y, Jin G, Xue Y, Wang D, Liu X, Sun J. Multifunctions of dual Zn/Mg ion co-implanted titanium on osteogenesis, angiogenesis and bacteria inhibition for dental implants. Acta Biomaterialia. 2017;49:590-603.

71. Gu Y, Zhang J, Zhang X, Liang G, Xu T, Niu W. Three-dimensional Printed Mg-Doped β-TCP Bone Tissue Engineering Scaffolds: Effects of Magnesium Ion Concentration on Osteogenesis and Angiogenesis *In Vitro*. Tissue Engineering and Regenerative Medicine. 2019;16(4):415-29.
72. Zhang X, Chen Q, Mao X. Magnesium Enhances Osteogenesis of BMSCs by Tuning Osteoimmunomodulation. BioMed Research International. 2019;2019.
73. Chen Z, Mao X, Tan L, Friis T, Wu C, Crawford R, et al. Osteoimmunomodulatory properties of magnesium scaffolds coated with β-tricalcium phosphate. Biomaterials. 2014;35(30):8553-65.
74. Negrescu A-M, Necula M-G, Gebaur A, Golgovici F, Nica C, Curti F, et al. *In Vitro* Macrophage Immunomodulation by Poly(ε-caprolactone) Based-Coated AZ31 Mg Alloy. International Journal of Molecular Sciences. 2021;22(2):909.
75. Zhou J, Sun S, Xu J, Yan T, He Y, Zhang L, et al. The magnesium-doped CSH/BCP promotes alveolar bone regeneration by mediating M2 macrophage polarization via miR-21–5p/Smad2 axis. Composites Part B: Engineering. 2024;287:111811.
76. Kanellopoulou C, George AB, Masutani E, Cannons JL, Ravell JC, Yamamoto TN, et al. Mg2+ regulation of kinase signaling and immune function. Journal of Experimental Medicine. 2019;216(8):1828-42.
77. Wang X, Li X, Ito A, Watanabe Y, Sogo Y, Hirose M, et al. Rod-shaped and substituted hydroxyapatite nanoparticles stimulating type 1 and 2 cytokine secretion. Colloids and Surfaces B: Biointerfaces. 2016;139:10-6.
78. Behrends JC, Bischofsberger, Josef, Deutzmann, Rainer. Duale Reihe Physiologie: Thieme; 2021.
79. Silbernagl SL, F. Taschenatlas Pathophysiologie2019.
80. Pape H-C, Kurtz, Armin, Silbernagl, Stefan, Klinke, Rainer Physiologie: Thieme; 2023.
81. Lüllmann-Rauch R. Taschenlehrbuch Histologie. 6., vollständig überarbeitete Auflage ed. Stuttgart New York: Georg Thieme Verlag; 2019.
82. Blum HE, Müller-Wieland, Dirk, Siegenthaler, Walter, Amann-Vesti, Beatrice. Klinische Pathophysiologie2020.

83. Physiologie des Menschen mit Pathophysiologie. 32. Auflage ed. Brandes R, Lang F, Schmidt RF, editors. Berlin: Springer; 2019.
84. Duale Reihe Innere Medizin. 5., vollständig überarbeitete Auflage ed. Stuttgart: Thieme; 2024.
85. Kalyan S, Quabius ES, Wiltfang J, Monig H, Kabelitz D. Can peripheral blood gammadelta T cells predict osteonecrosis of the jaw? An immunological perspective on the adverse drug effects of aminobisphosphonate therapy. J Bone Miner Res. 2013;28(4):728-35.
86. Lieberman SM, Evans AM, Han B, Takaki T, Vinnitskaya Y, Caldwell JA, et al. Identification of the beta cell antigen targeted by a prevalent population of pathogenic CD8+ T cells in autoimmune diabetes. Proc Natl Acad Sci U S A. 2003;100(14):8384-8.
87. Wang M, Tian T, Yu S, He N, Ma D. Th17 and Treg cells in bone related diseases. Clin Dev Immunol. 2013;2013:203705.
88. Lam J, Takeshita S, Barker JE, Kanagawa O, Ross FP, Teitelbaum SL. TNF-alpha induces osteoclastogenesis by direct stimulation of macrophages exposed to permissive levels of RANK ligand. J Clin Invest. 2000;106(12):1481-8.
89. Ross SH, Cantrell DA. Signaling and Function of Interleukin-2 in T Lymphocytes. Annual Review of Immunology. 2018;36(Volume 36, 2018):411-33.
90. Srivastava RK, Dar HY, Mishra PK. Immunoporosis: Immunology of Osteoporosis-Role of T Cells. Front Immunol. 2018;9:657.
91. Breuil V, Ticchioni M, Testa J, Roux CH, Ferrari P, Breittmayer JP, et al. Immune changes in post-menopausal osteoporosis: the Immunos study. Osteoporos Int. 2010;21(5):805-14.
92. Masuzawa T, Miyaura C, Onoe Y, Kusano K, Ohta H, Nozawa S, et al. Estrogen deficiency stimulates B lymphopoiesis in mouse bone marrow. The Journal of Clinical Investigation. 1994;94(3):1090-7.
93. Onal M, Xiong J, Chen X, Thostenson JD, Almeida M, Manolagas SC, et al. Receptor activator of nuclear factor kappaB ligand (RANKL) protein expression by B lymphocytes contributes to ovariectomy-induced bone loss. J Biol Chem. 2012;287(35):29851-60.

94. Weitzmann MN. The Role of Inflammatory Cytokines, the RANKL/OPG Axis, and the Immunoskeletal Interface in Physiological Bone Turnover and Osteoporosis. Scientifica (Cairo). 2013;2013:125705.
95. Zhang Z, Yuan W, Deng J, Wang D, Zhang T, Peng L, et al. Granulocyte colony stimulating factor (G-CSF) regulates neutrophils infiltration and periodontal tissue destruction in an experimental periodontitis. Mol Immunol. 2020;117:110-21.
96. Frase D, Lee C, Nachiappan C, Gupta R, Akkouch A. The Inflammatory Contribution of B-Lymphocytes and Neutrophils in Progression to Osteoporosis. Cells. 2023;12(13).
97. Huang C, Li S. Association of blood neutrophil lymphocyte ratio in the patients with postmenopausal osteoporosis. Pak J Med Sci. 2016;32(3):762-5.
98. Fischer V, Haffner-Luntzer M. Interaction between bone and immune cells: Implications for postmenopausal osteoporosis. Semin Cell Dev Biol. 2022;123:14-21.
99. Chaney S, Vergara R, Qiryaqoz Z, Suggs K, Akkouch A. The Involvement of Neutrophils in the Pathophysiology and Treatment of Osteoarthritis. Biomedicines. 2022;10(7).
100. Saxena Y, Routh S, Mukhopadhaya A. Immunoporosis: Role of Innate Immune Cells in Osteoporosis. Front Immunol. 2021;12:687037.
101. Ginaldi L, De Martinis M, Ciccarelli F, Saitta S, Imbesi S, Mannucci C, et al. Increased levels of interleukin 31 (IL-31) in osteoporosis. BMC Immunol. 2015;16:60.
102. Andreev D, Kachler K, Liu M, Chen Z, Krishnacoumar B, Ringer M, et al. Eosinophils preserve bone homeostasis by inhibiting excessive osteoclast formation and activity via eosinophil peroxidase. Nat Commun. 2024;15(1):1067.
103. Michalski MN, McCauley LK. Macrophages and skeletal health. Pharmacol Ther. 2017;174:43-54.
104. Horwood NJ. Macrophage Polarization and Bone Formation: A review. Clin Rev Allergy Immunol. 2016;51(1):79-86.
105. Gong L, Zhao Y, Zhang Y, Ruan Z. The Macrophage Polarization Regulates MSC Osteoblast Differentiation *in vitro*. Ann Clin Lab Sci. 2016;46(1):65-71.
106. Zhang Y, Bose T, Unger RE, Jansen JA, Kirkpatrick CJ, van den Beucken J. Macrophage type modulates osteogenic differentiation of adipose tissue MSCs. Cell Tissue Res. 2017;369(2):273-86.

107. Yang DH, Yang MY. The Role of Macrophage in the Pathogenesis of Osteoporosis. Int J Mol Sci. 2019;20(9).
108. Dou C, Ding N, Zhao C, Hou T, Kang F, Cao Z, et al. Estrogen Deficiency-Mediated M2 Macrophage Osteoclastogenesis Contributes to M1/M2 Ratio Alteration in Ovariectomized Osteoporotic Mice. J Bone Miner Res. 2018;33(5):899-908.
109. Murray PJ. Macrophage Polarization. Annu Rev Physiol. 2017;79:541-66.
110. Holweg P, Labmayr V, Schwarze U, Sommer NG, Ornig M, Leithner A. Osteotomy after medial malleolus fracture fixed with magnesium screws ZX00 - A case report. Trauma Case Rep. 2022;42:100706.
111. Holweg P, Berger L, Cihova M, Donohue N, Clement B, Schwarze U, et al. A lean magnesium-zinc-calcium alloy ZX00 used for bone fracture stabilization in a large growing-animal model. Acta Biomater. 2020;113:646-59.
112. Sommer NG, Hirzberger D, Paar L, Berger L, Cwieka H, Schwarze UY, et al. Implant degradation of low-alloyed Mg-Zn-Ca in osteoporotic, old and juvenile rats. Acta Biomater. 2022;147:427-38.
113. Manolagas SC, Jilka RL. Bone marrow, cytokines, and bone remodeling—emerging insights into the pathophysiology of osteoporosis. New England journal of medicine. 1995;332(5):305-11.
114. Riggs BL, Melton LJ. The Prevention and Treatment of Osteoporosis. New England Journal of Medicine. 1992;327(9):620-7.
115. Pesce V, Speciale D, Sammarco G, Patella S, Spinarelli A, Patella V. Surgical approach to bone healing in osteoporosis. Clin Cases Miner Bone Metab. 2009;6(2):131-5.
116. Wang J, Tang J, Zhang P, Li Y, Wang J, Lai Y, et al. Surface modification of magnesium alloys developed for bioabsorbable orthopedic implants: A general review. Journal of Biomedical Materials Research Part B: Applied Biomaterials. 2012;100B(6):1691-701.
117. Okutan B, Schwarze UY, Berger L, Martinez DC, Herber V, Suljevic O, et al. The combined effect of zinc and calcium on the biodegradation of ultrahigh-purity magnesium implants. Biomaterials Advances. 2023;146:213287.

118. Holweg P, Berger L, Cihova M, Donohue N, Clement B, Schwarze U, et al. A lean magnesium-zinc-calcium alloy ZX00 used for bone fracture stabilization in a large growing-animal model. Acta Biomater. 2020;113:646-59.
119. Rahmati M, Stotzel S, Khassawna TE, Iskhahova K, Florian Wieland DC, Zeller Plumhoff B, et al. Early osteoimmunomodulatory effects of magnesium-calcium-zinc alloys. J Tissue Eng. 2021;12:20417314211047100.
120. Marek R, Cwieka H, Donohue N, Holweg P, Moosmann J, Beckmann F, et al. Degradation behavior and osseointegration of Mg-Zn-Ca screws in different bone regions of growing sheep: a pilot study. Regen Biomater. 2023;10:rbac077.
121. Martinez DC, Dobkowska A, Marek R, Cwieka H, Jaroszewicz J, Plocinski T, et al. *In vitro* and *in vivo* degradation behavior of Mg-0.45Zn-0.45Ca (ZX00) screws for orthopedic applications. Bioact Mater. 2023;28:132-54.
122. Jee WS, Yao W. Overview: animal models of osteopenia and osteoporosis. J Musculoskelet Neuronal Interact. 2001;1(3):193-207.
123. Erben RG. Trabecular and endocortical bone surfaces in the rat: Modeling or remodeling? The Anatomical Record. 1996;246(1):39-46.
124. Bouxsein ML, Boyd SK, Christiansen BA, Guldberg RE, Jepsen KJ, Muller R. Guidelines for assessment of bone microstructure in rodents using micro-computed tomography. J Bone Miner Res. 2010;25(7):1468-86.
125. Boyd SK, Davison P, Müller R, Gasser JA. Monitoring individual morphological changes over time in ovariectomized rats by *in vivo* micro-computed tomography. Bone. 2006;39(4):854-62.
126. Gao X, Ma W, Dong H, Yong Z, Su R. Establishing a rapid animal model of osteoporosis with ovariectomy plus low calcium diet in rats. Int J Clin Exp Pathol. 2014;7(8):5123-8.
127. Abildgaard J, Tingstedt J, Zhao Y, Hartling HJ, Pedersen AT, Lindegaard B, et al. Increased systemic inflammation and altered distribution of T-cell subsets in postmenopausal women. PLoS One. 2020;15(6):e0235174.
128. Wu D, Cline-Smith A, Shashkova E, Perla A, Katyal A, Aurora R. T-Cell Mediated Inflammation in Postmenopausal Osteoporosis. Front Immunol. 2021;12:687551.

129. Nordqvist J, Bernardi A, Islander U, Carlsten H. Effects of a tissue-selective estrogen complex on B lymphopoiesis and B cell function. Immunobiology. 2017;222(8):918-23.
130. Mansour A, Anginot A, Mancini SJC, Schiff C, Carle GF, Wakkach A, et al. Osteoclast activity modulates B-cell development in the bone marrow. Cell Research. 2011;21(7):1102-15.
131. Chen L, Yang L, Yao M, Cui XJ, Xue CC, Wang YJ, et al. Biomechanical Characteristics of Osteoporotic Fracture Healing in Ovariectomized Rats: A Systematic Review. PLoS One. 2016;11(4):e0153120.
132. He Y-X, Zhang G, Pan X-H, Liu Z, Zheng L-z, Chan C-W, et al. Impaired bone healing pattern in mice with ovariectomy-induced osteoporosis: A drill-hole defect model. Bone. 2011;48(6):1388-400.
133. Wong R, Thormann U, Choy M, Chim N, Li M, Wang J, et al. A metaphyseal fracture rat model for mechanistic studies of osteoporotic bone healing. European cells & materials. 2019;37:420-30.
134. Zhang Y, Xu J, Ruan YC, Yu MK, O'Laughlin M, Wise H, et al. Implant-derived magnesium induces local neuronal production of CGRP to improve bone-fracture healing in rats. Nature Medicine. 2016;22(10):1160-9.
135. Galli S, Stocchero M, Andersson M, Karlsson J, He W, Lilin T, et al. The effect of magnesium on early osseointegration in osteoporotic bone: a histological and gene expression investigation. Osteoporosis International. 2017;28:2195 - 205.
136. Li X, Li Y, Liao Y, Li J, Zhang L, Hu J. The effect of magnesium-incorporated hydroxyapatite coating on titanium implant fixation in ovariectomized rats. Int J Oral Maxillofac Implants. 2014;29(1):196-202.
137. Yamakawa K, Tajima G, Keegan JW, Nakahori Y, Guo F, Seshadri AJ, et al. Trauma induces expansion and activation of a memory-like Treg population. J Leukoc Biol. 2021;109(3):645-56.
138. Peng Y, Yang J, Fu W, Gao Q, Yao S, Peng C, et al. Osteoimmunomodulatory properties of a magnesium-doped phase-transited lysozyme coating on titanium. Materials Today Advances. 2022;14:100234.
139. Nish SA, Schenten D, Wunderlich FT, Pope SD, Gao Y, Hoshi N, et al. T cell-intrinsic role of IL-6 signaling in primary and memory responses. Elife. 2014;3:e01949.

140. Shao BY, Wang L, Yu Y, Chen L, Gan N, Huang WM. Effects of CD4(+) T lymphocytes from ovariectomized mice on bone marrow mesenchymal stem cell proliferation and osteogenic differentiation. Exp Ther Med. 2020;20(5):84.
141. Riyaz S, Sun Y, Helmholz H, Medina TP, Medina OP, Wiese B, et al. Inflammatory response toward a Mg-based metallic biomaterial implanted in a rat femur fracture model. Acta Biomaterialia. 2024;185:41-54.
142. Castellani C, Lindtner RA, Hausbrandt P, Tschegg E, Stanzl-Tschegg SE, Zanoni G, et al. Bone–implant interface strength and osseointegration: Biodegradable magnesium alloy versus standard titanium control. Acta Biomaterialia. 2011;7(1):432-40.
143. Zhang E, Xu L, Yu G, Pan F, Yang K. *In vivo* evaluation of biodegradable magnesium alloy bone implant in the first 6 months implantation. Journal of Biomedical Materials Research Part A. 2009;90A(3):882-93.